Supporting information for:

Exploring the limits of adsorption-based CO_2 capture using MOFs with PVSA – from molecular design to process economics

David Danaci[a,b], Mai Bui[c,d], Niall Mac Dowell[c,d], Camille Petit[a,b]

a – Department of Chemical Engineering, Imperial College London, SW7 2AZ, UK

b – Barrer Centre, Imperial College London, SW7 2AZ, UK

c – Centre for Environmental Polity, Imperial College London, SW7 1NE, UK

d – Centre for Process Systems Engineering, Imperial College London, SW7 2AZ, UK

Table of contents

Table of figures

Supplementary results

Figures and results accompanying the discussion in the main body.

Capital cost breakdowns

Breakdown of capital costs for each scenario, at 0.15 bar_a desorption pressure.

Natural gas

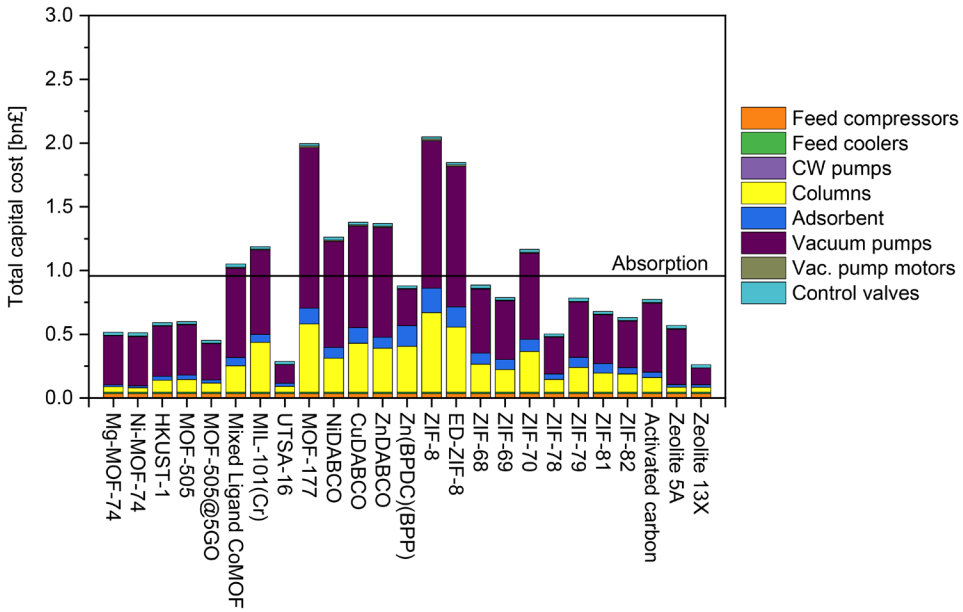

Figure 1 – Capital cost breakdown for each adsorbent for the natural gas scenario at 0.15 bar_a desorption pressure

Coal

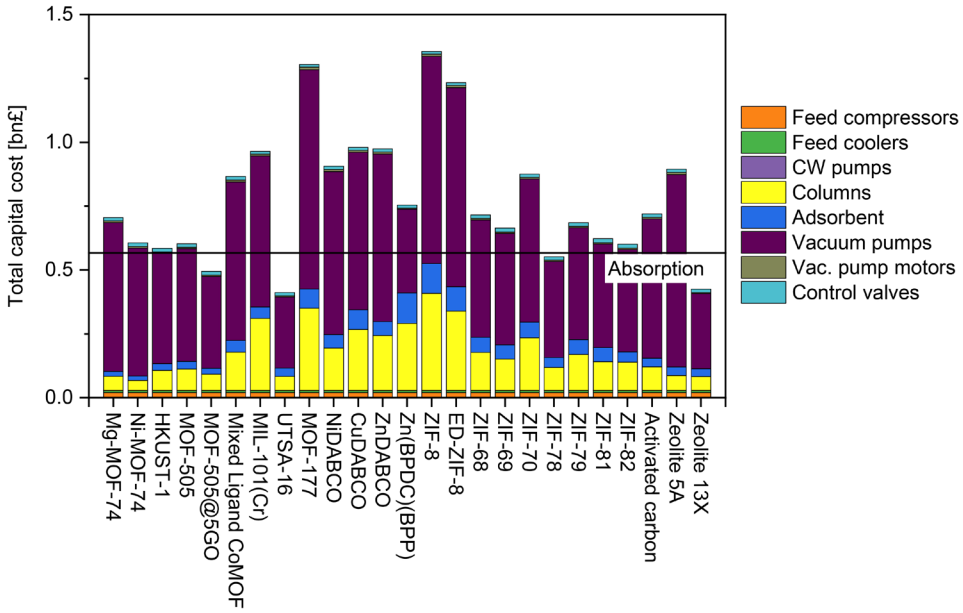

Figure 2 – Capital cost breakdown for each adsorbent for the coal scenario at 0.15 bar_a desorption pressure

Cement

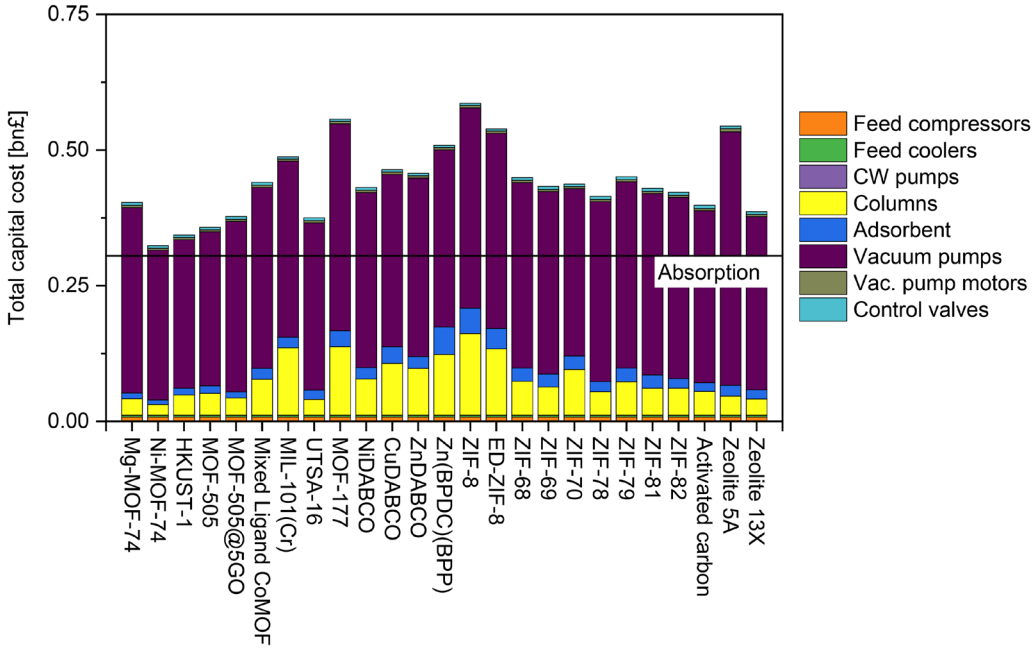

Figure 3 – Capital cost breakdown for each adsorbent for the cement scenario at 0.15 bar_a desorption pressure

Steel

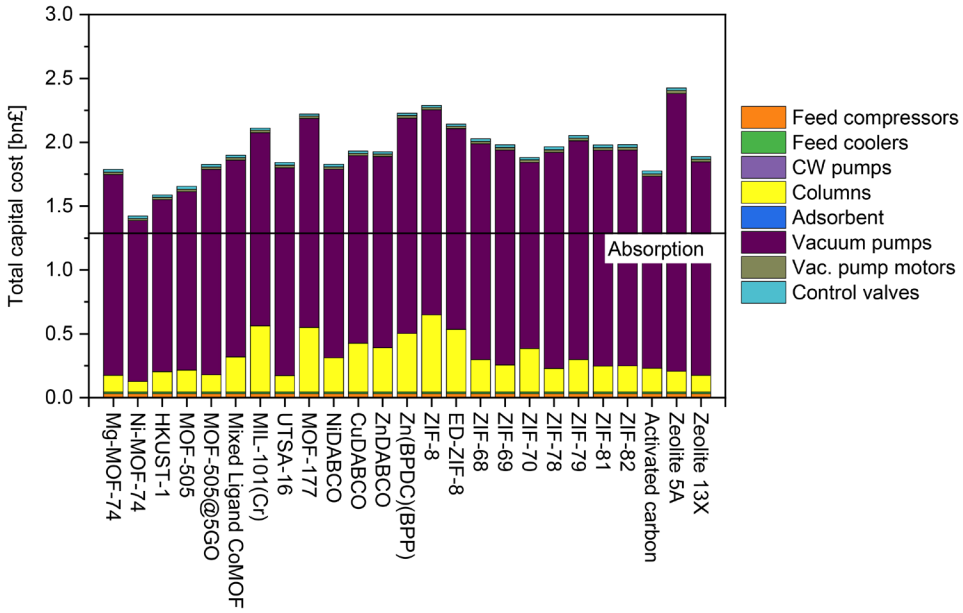

Figure 4 – Capital cost breakdown for each adsorbent for the steel scenario at 0.15 bar_a desorption pressure

Energy penalty plots

Plots showing the total electrical energy penalty, and the specific energy requirements for each scenario are presented here.

Natural gas

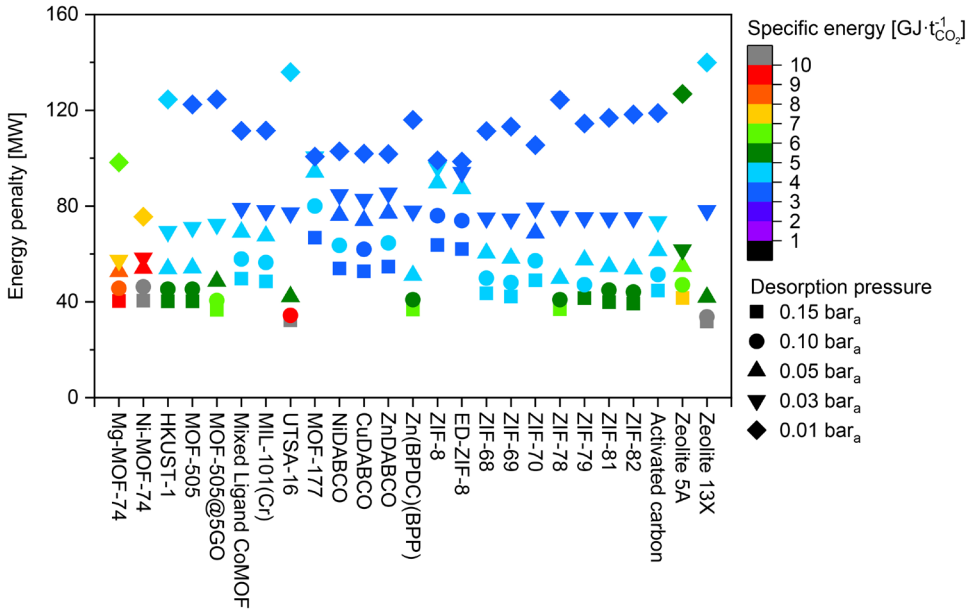

Figure 5 – Energy penalty and specific energy consumption for the natural gas scenario

Coal

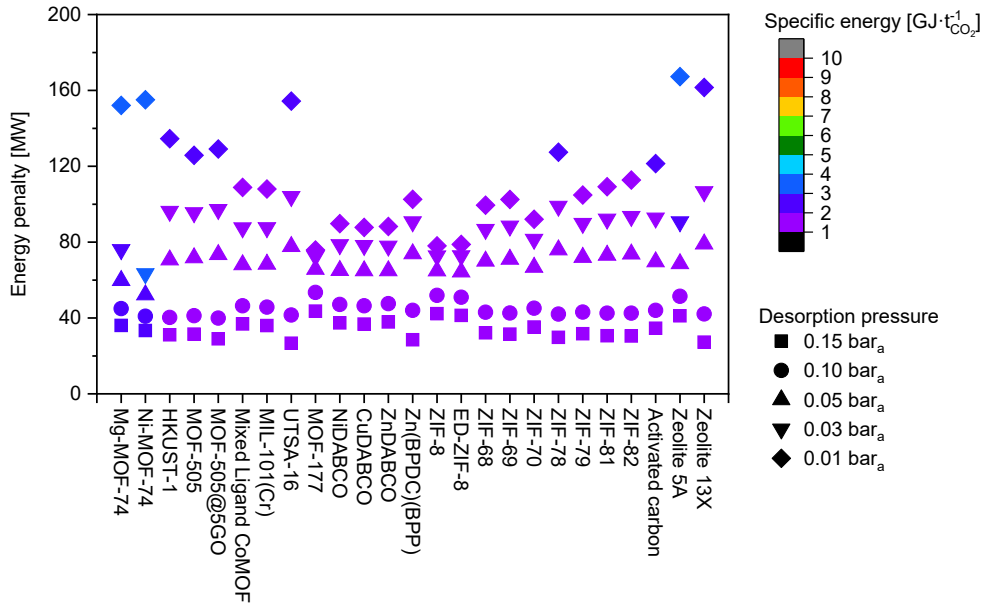

Figure 6 – Energy penalty and specific energy consumption for the coal scenario

Cement

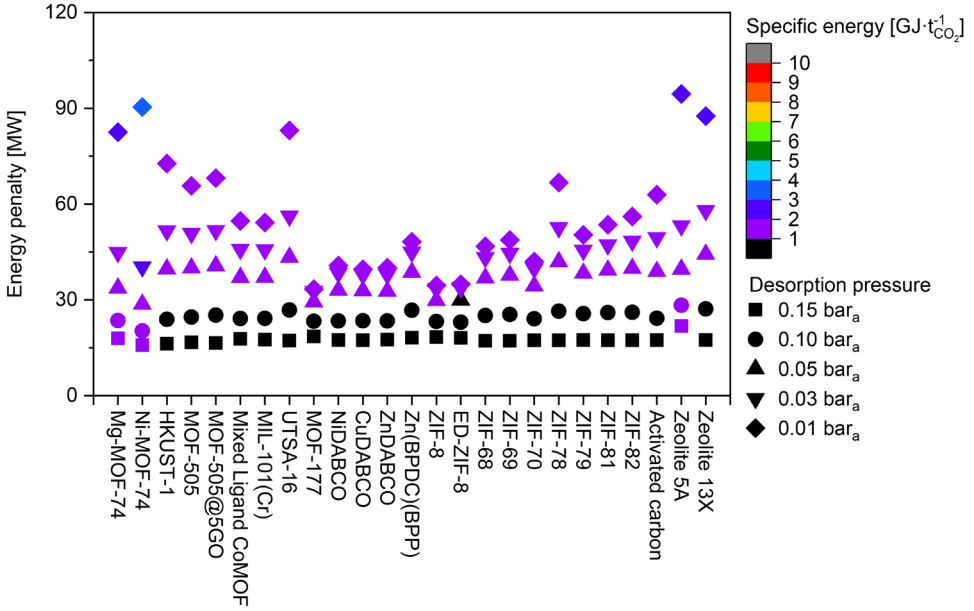

Figure 7 – Energy penalty and specific energy consumption for the cement scenario

Steel

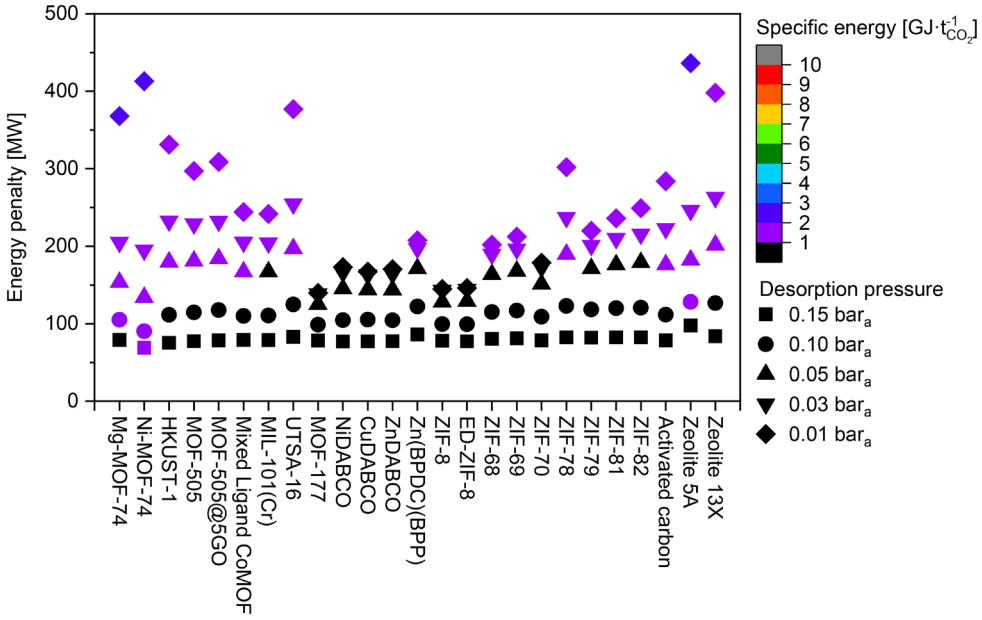

Figure 8 – Energy penalty and specific energy consumption for the steel scenario

Working selectivity

Plots of the working selectivity of each adsorbent for each of the scenarios are presented here.

The working selectivity is the ratio of the working capacity of CO_2 to N_2.

Natural gas

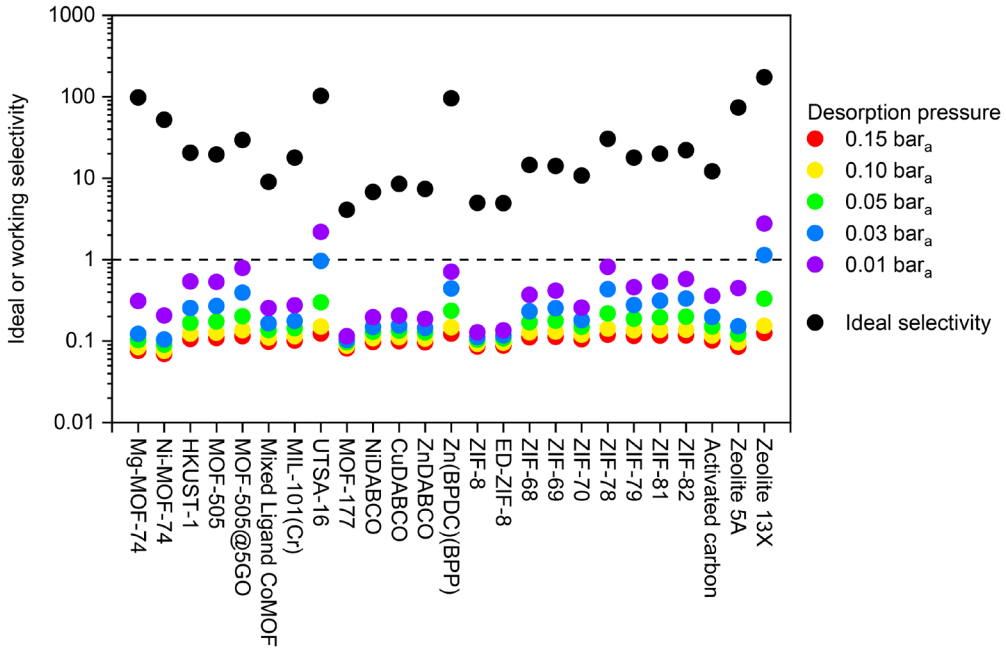

Figure 9 – Working and ideal selectivities for the natural gas scenario

Coal

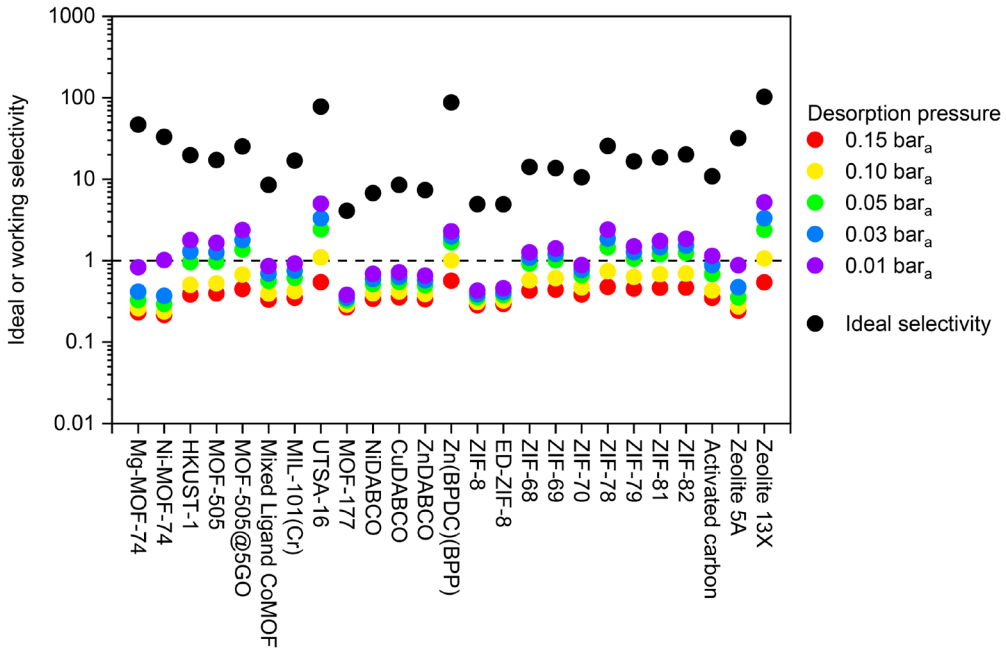

Figure 10 – Working and ideal selectivities for the coal scenario

Cement

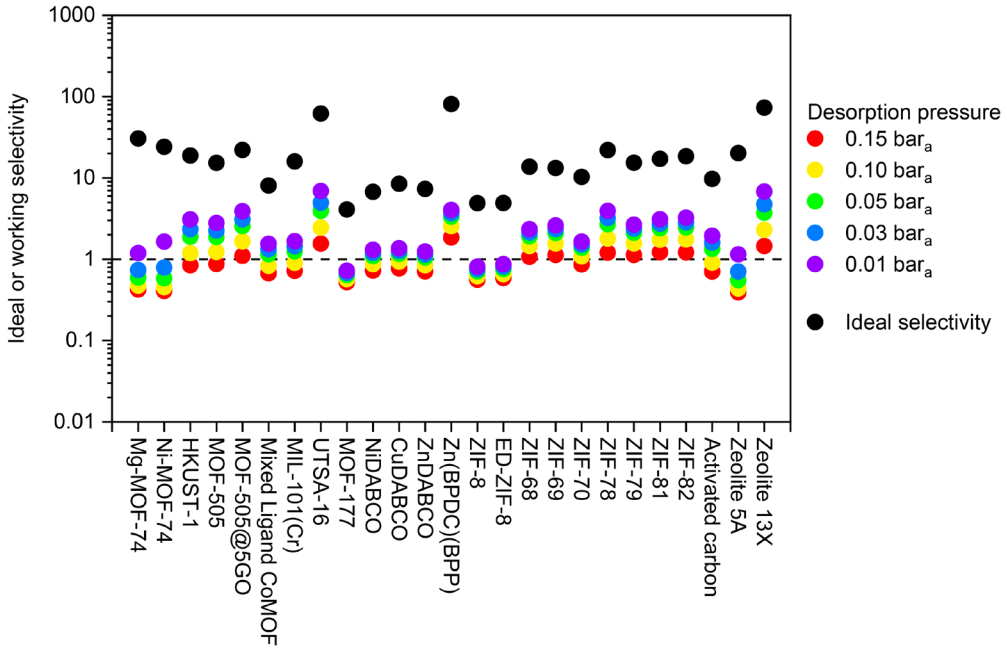

Figure 11 – Working and ideal selectivities for the cement scenario

Steel

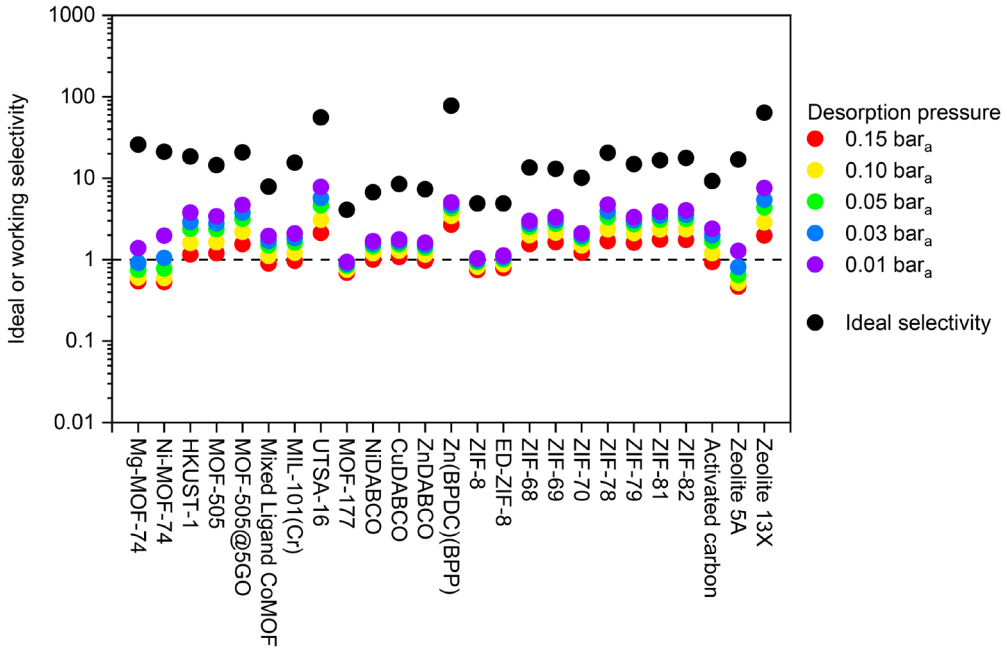

Figure 12 – Working and ideal selectivities for the steel scenario

Sensitivity analysis

The sensitivity analysis plots for purity, recovery, and cost are presented here for Mg-MOF-74 and UTSA-16 at 0.01 bara desorption pressure for the natural gas scenario.

Purity

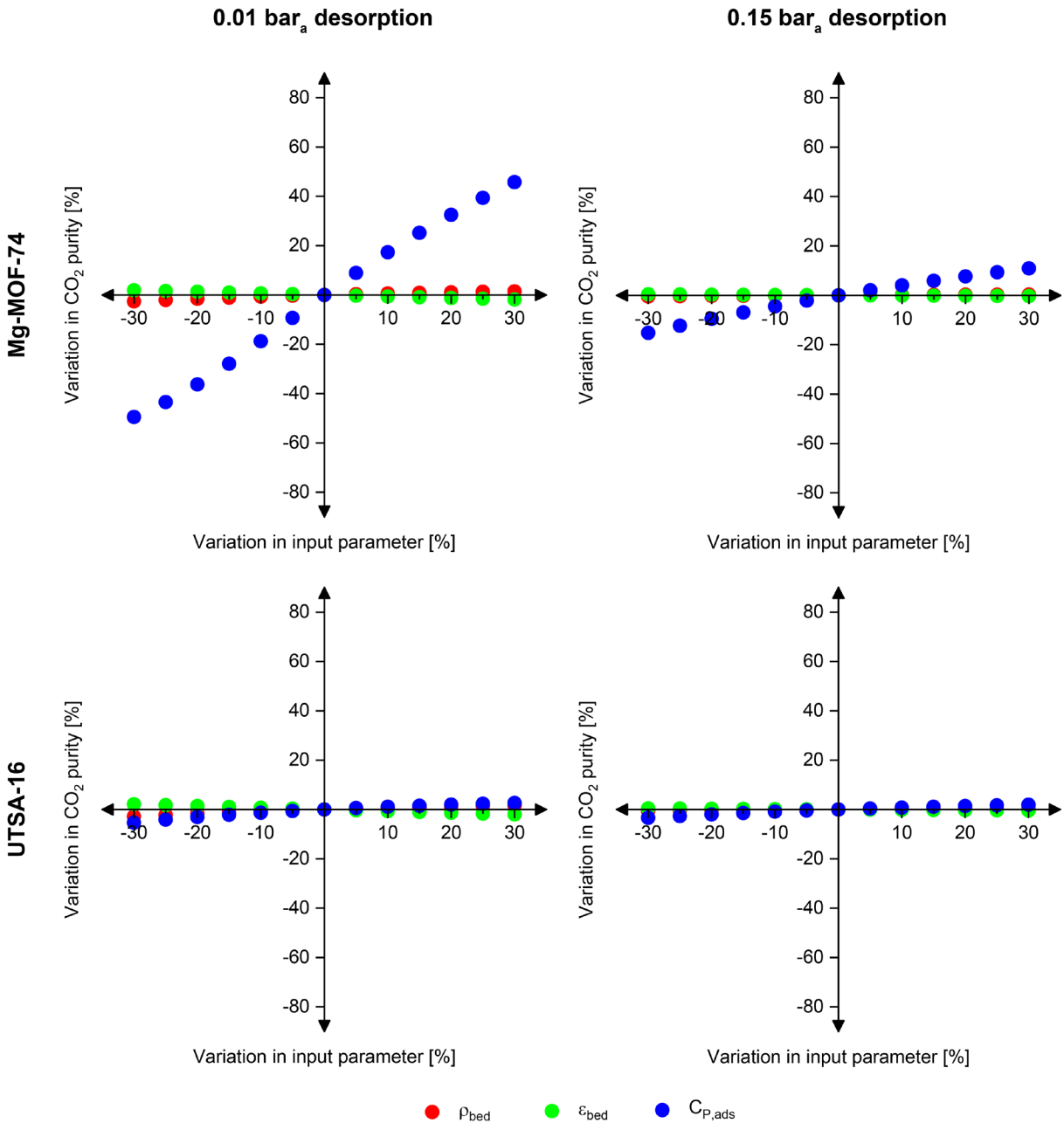

Figure 13 – Sensitivity analysis of density, void fraction, and heat capacity for Mg-MOF-74 and UTSA-16 at 0.01 bar$_a$ and 0.15 bar$_a$ desorption pressure on CO_2 purity

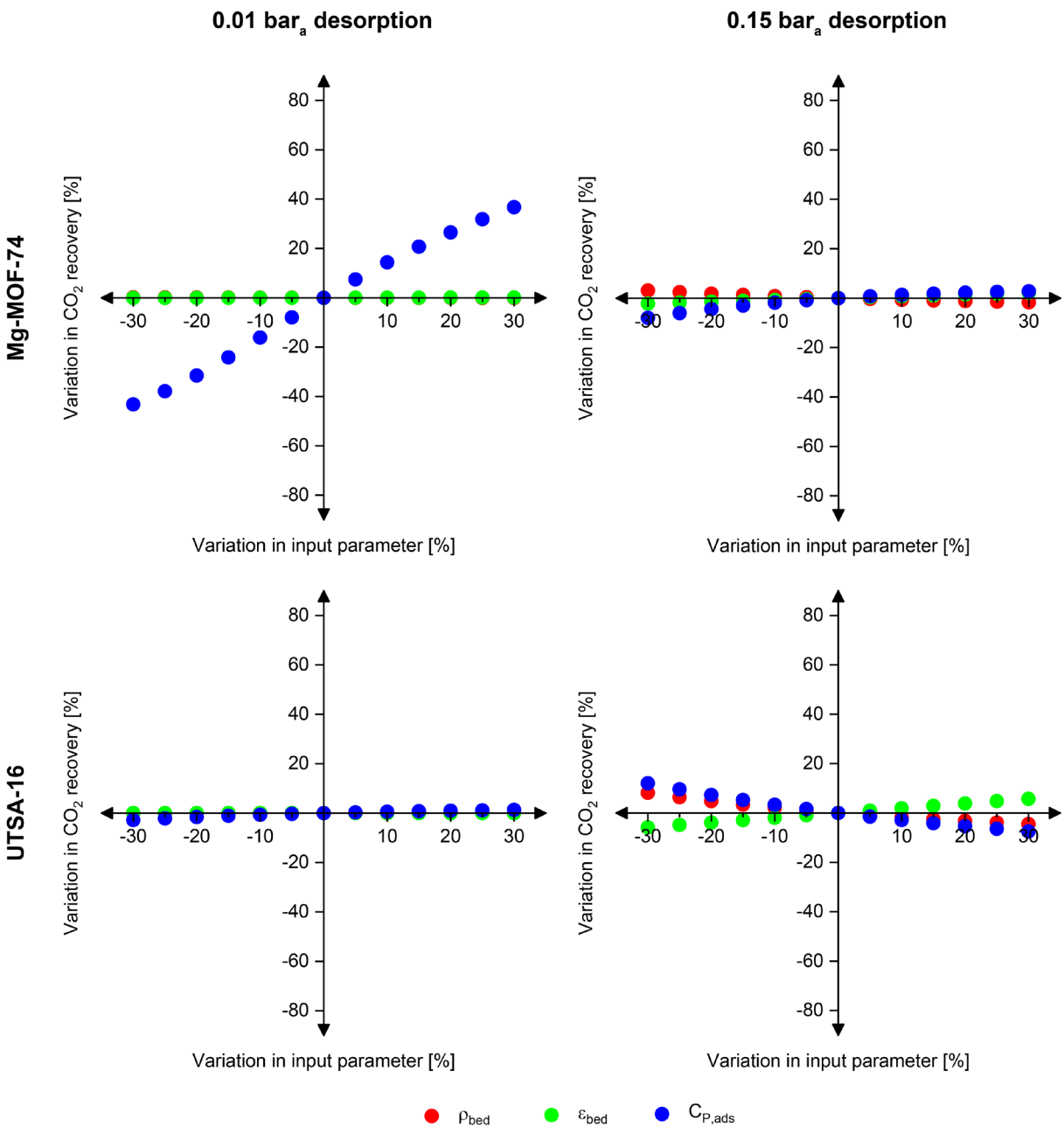

Figure 14 – Sensitivity analysis of density, void fraction, and heat capacity for Mg-MOF-74 and UTSA-16 at 0.01 bar$_a$ and 0.15 bar$_a$ desorption pressure on CO_2 recovery

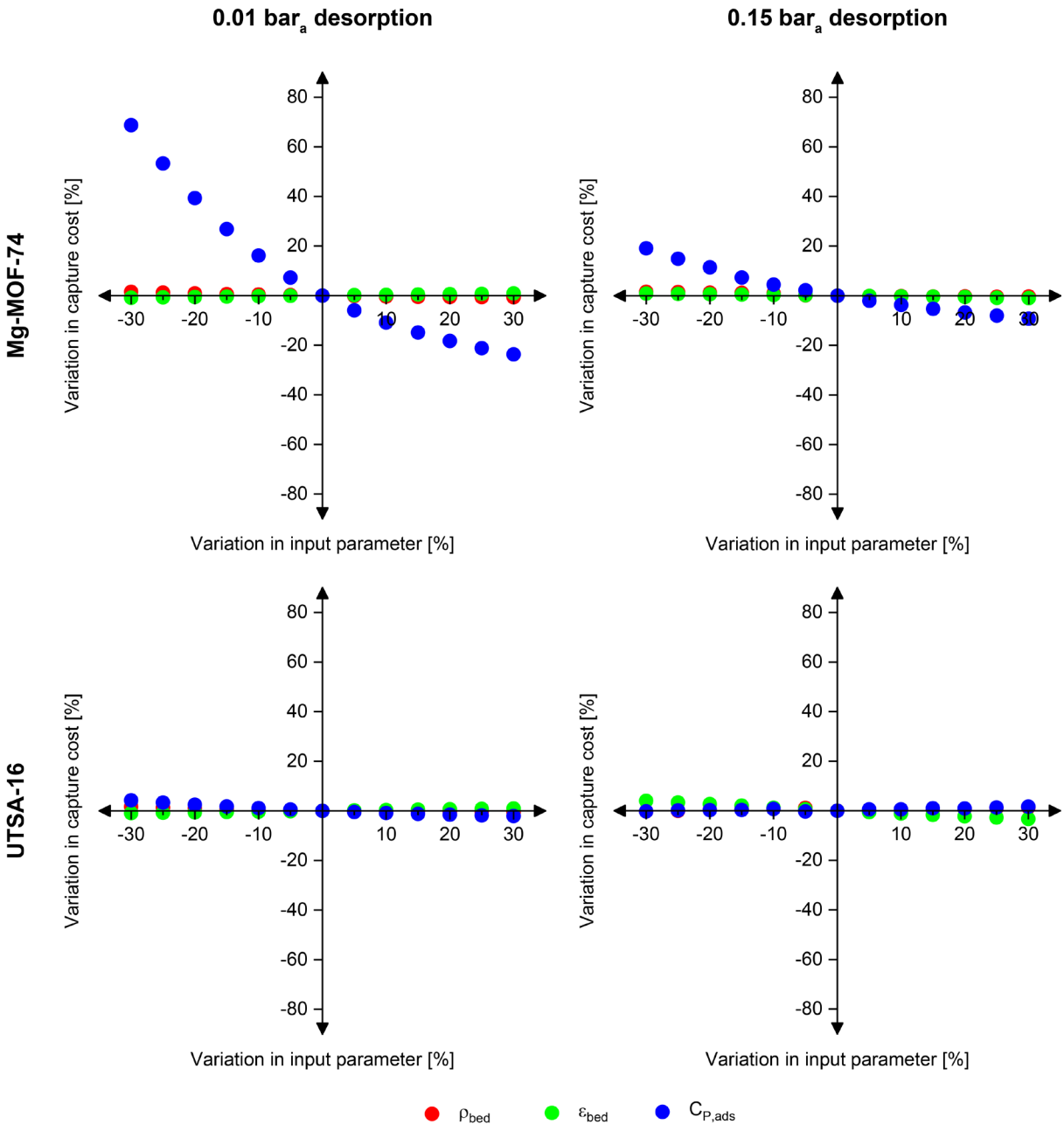

Figure 15 – Sensitivity analysis of density, void fraction, and heat capacity for Mg-MOF-74 and UTSA-16 at 0.01 bar$_a$ and 0.15 bar$_a$ desorption pressure on CO_2 capture cost

Effect of adsorption temperature (extended range)

Plots of purity and recovery are provided for all adsorbents over a wider temperature range for the natural gas scenario.

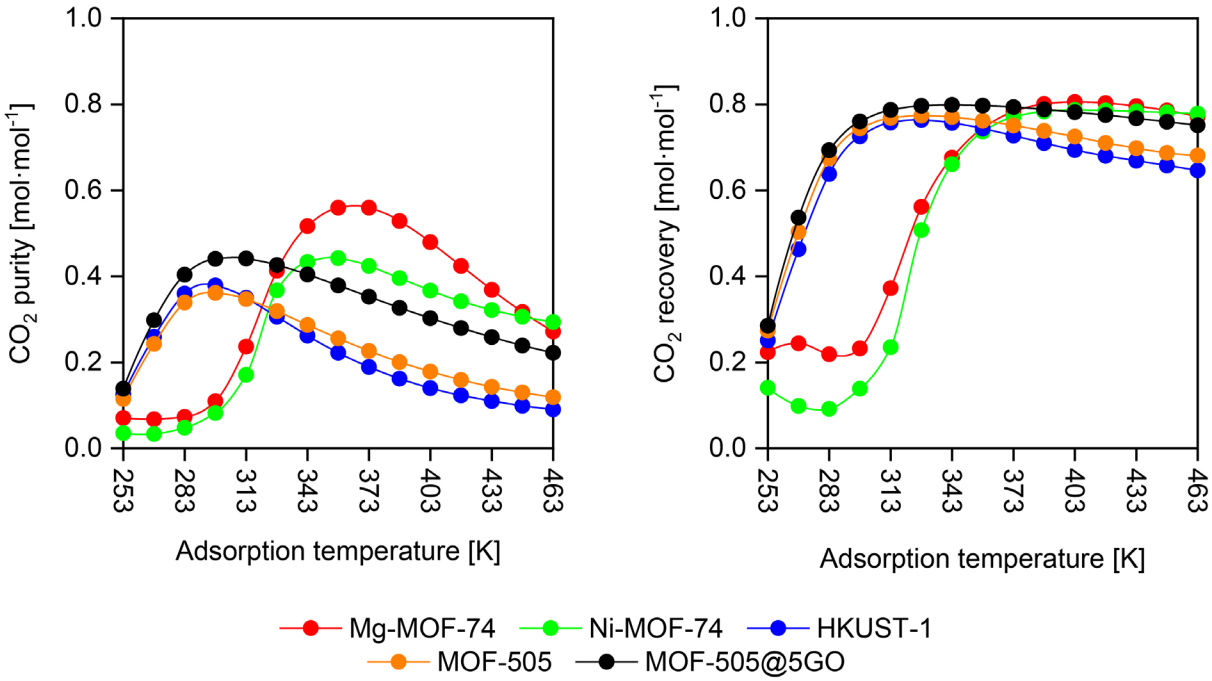

Figure 16 – Effect of adsorption temperature on CO_2 purity and recovery for Mg-MOF-74, Ni-MOF-74, HKUST-1, MOF-505, and MOF-505@GO

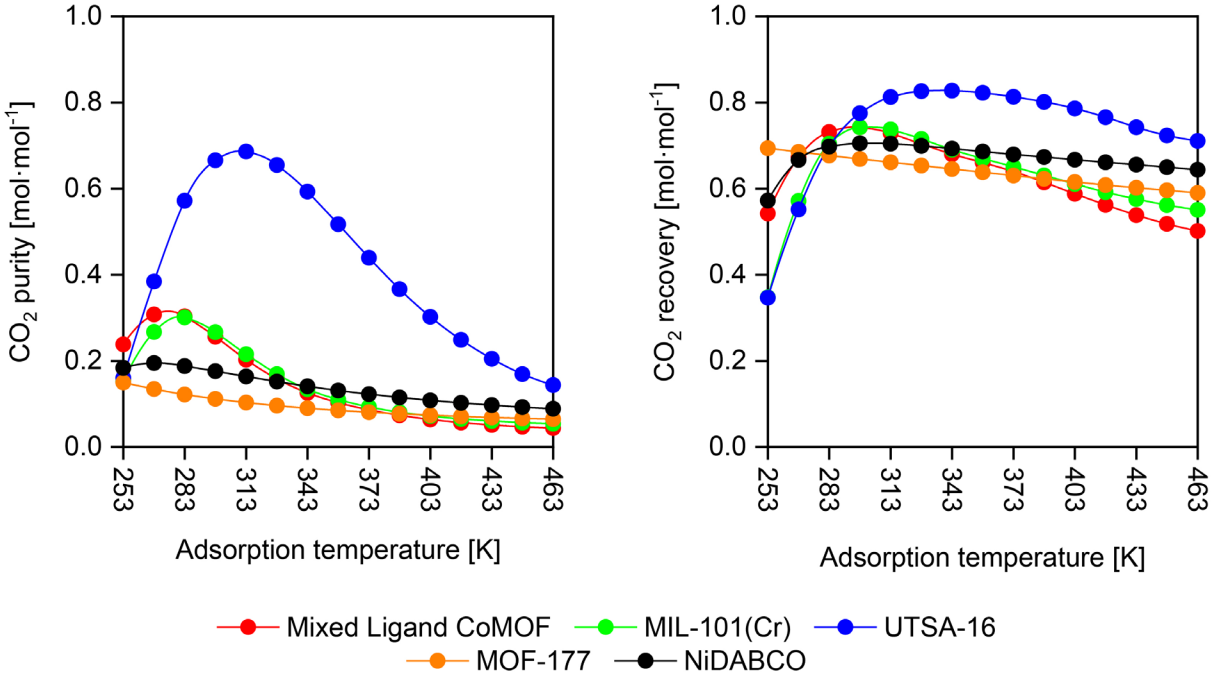

Figure 17 – Effect of adsorption temperature on CO_2 purity and recovery for Mixed Ligand CoMOF, MIL-101(Cr), UTSA-16, MOF-177, and NiDABCO

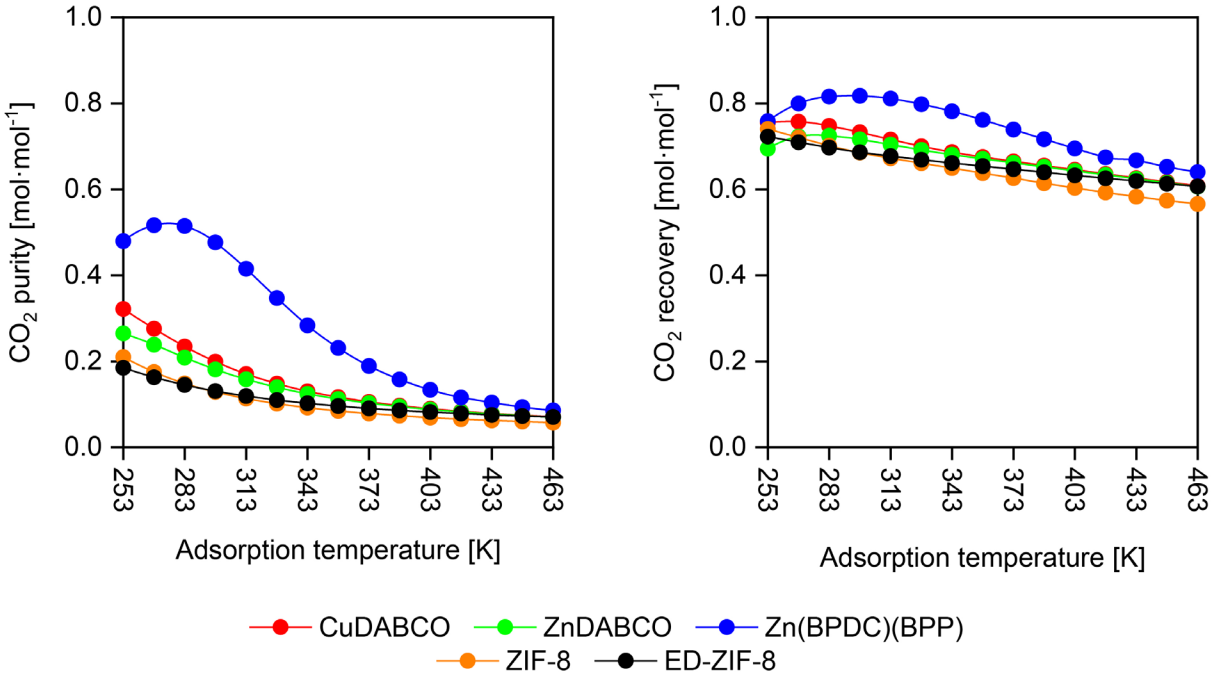

Figure 18 – Effect of adsorption temperature on CO_2 purity and recovery for CuDABCO, ZnDABCO, Zn(BPDC)(BPP), ZIF-8, and ED-ZIF-8

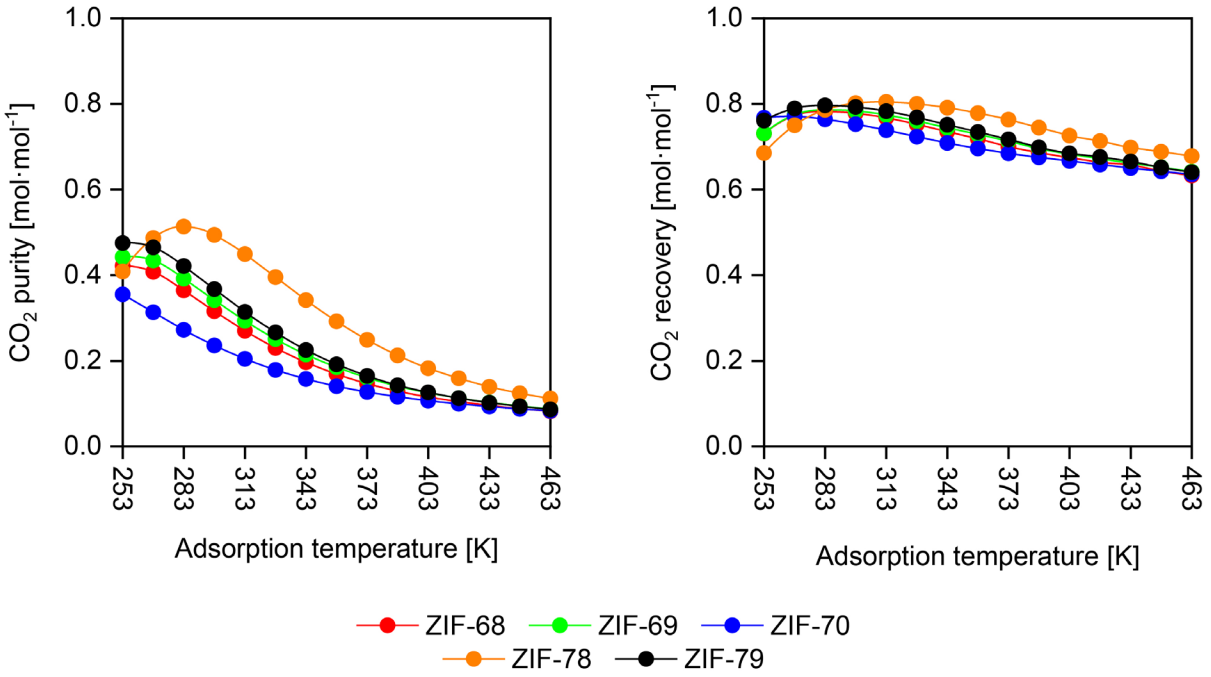

Figure 19 – Effect of adsorption temperature on CO_2 purity and recovery for ZIF-68, ZIF-69, ZIF-70, ZIF-78, and ZIF-79

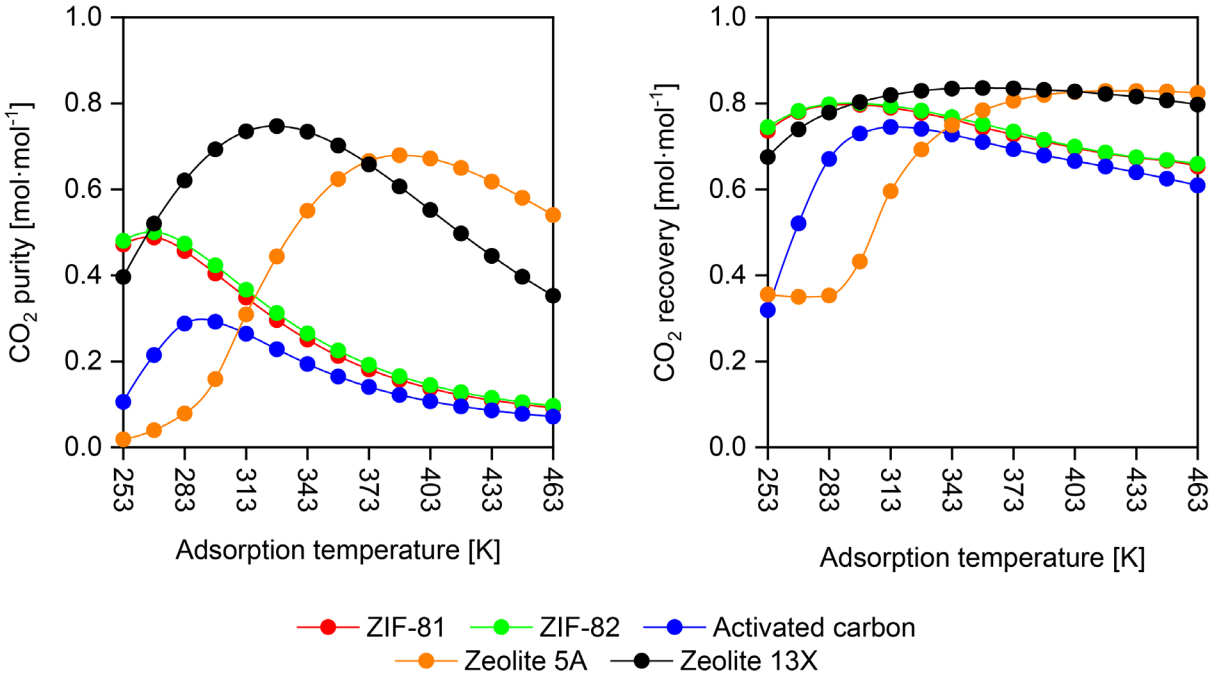

Figure 20 – Effect of adsorption temperature on CO_2 purity and recovery for ZIF-81, ZIF-82, activated carbon, zeolite 5A, and zeolite 13X

Operating cost fractions

Fraction of operating cost relative to total annual cost, for all adsorbents, for the natural gas scenario.

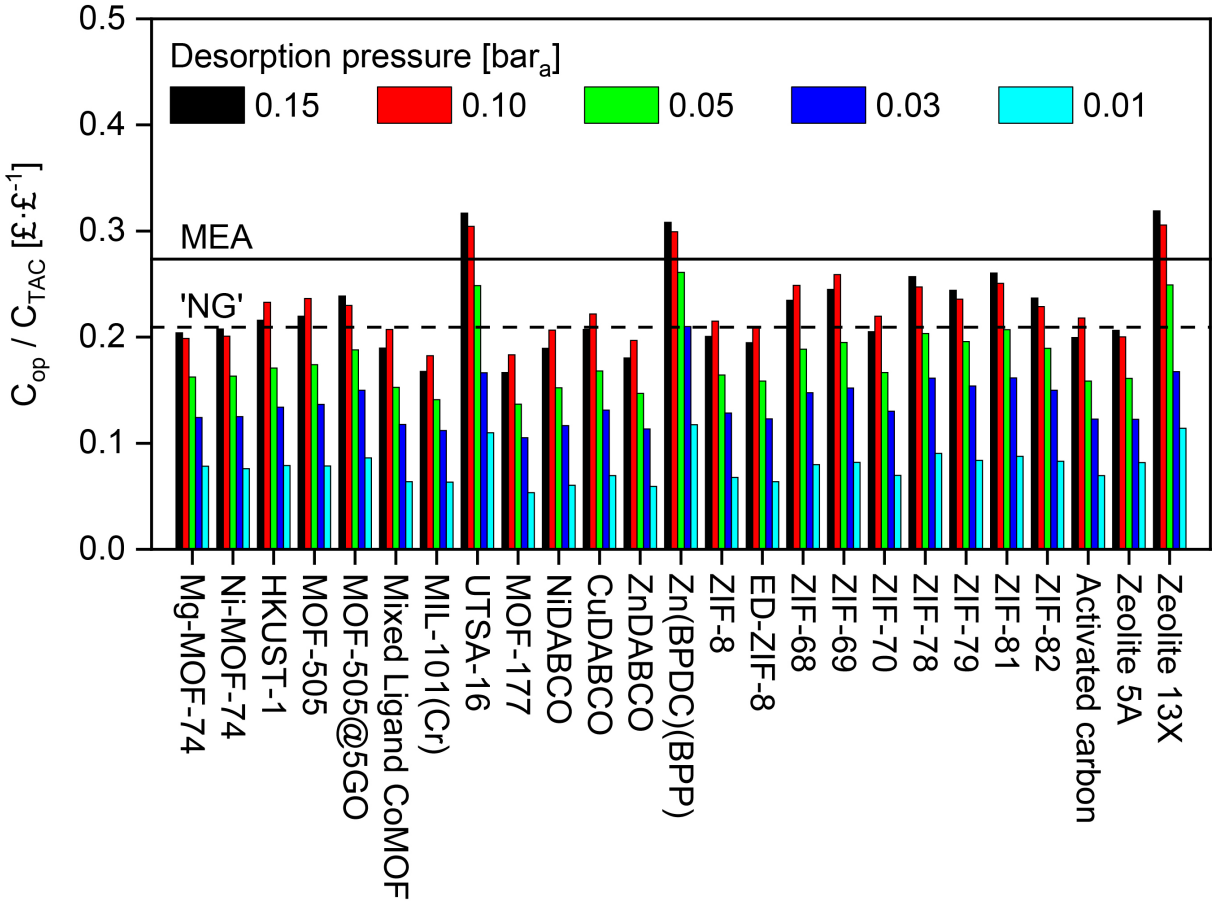

Figure 21 – Proportion of total annual costs that are operating costs at each desorption pressure for the natural gas scenario for each adsorbent

Surrogate model goodness-of-fit

The goodness of fit metrics for the surrogate model are provided here. Statistical analysis is also provided on the values of the absolute and percentage errors.

The parameters are defined as below, where y_a is the 'actual value' or 'input value', and y_f is the 'fitted value' or 'predicted value'.

$$\text{Residual} = y_f - y_a$$

$$\text{Err}_{\text{absolute}} = \left| y_f - y_a \right|$$

$$\text{Err}_{\text{percentage}} = \left| \frac{y_f - y_a}{y_a} \right| \times 100$$

Absolute error statistics

Number of points	Number of input points to model	
Minimum	Minimum value of $\text{Err}_{\text{absolute}}$	[units]
Maximum	Maximum value of $\text{Err}_{\text{absolute}}$	
Average	Average value of $\text{Err}_{\text{absolute}}$	
Median	Median value of $\text{Err}_{\text{absolute}}$	
Standard deviation	Standard deviation of $\text{Err}_{\text{absolute}}$	
Margin of error for 99 % confidence interval	99 % confidence interval based on standard error.	

The percentage error statistic table shows the number of points (and the corresponding percentage of the total number of points) of the dataset that have percentage errors greater than the indicated value. The table is not bounded, i.e. if 17 points have a percentage error greater than 5 %, and 4 points greater than 10 %, there are 13 points between 5 and 10 %.

Percentage error statistics

Percentage error	Number of points greater than	Percentage of total points
5		
10		
15		
20		

Natural gas

Purity

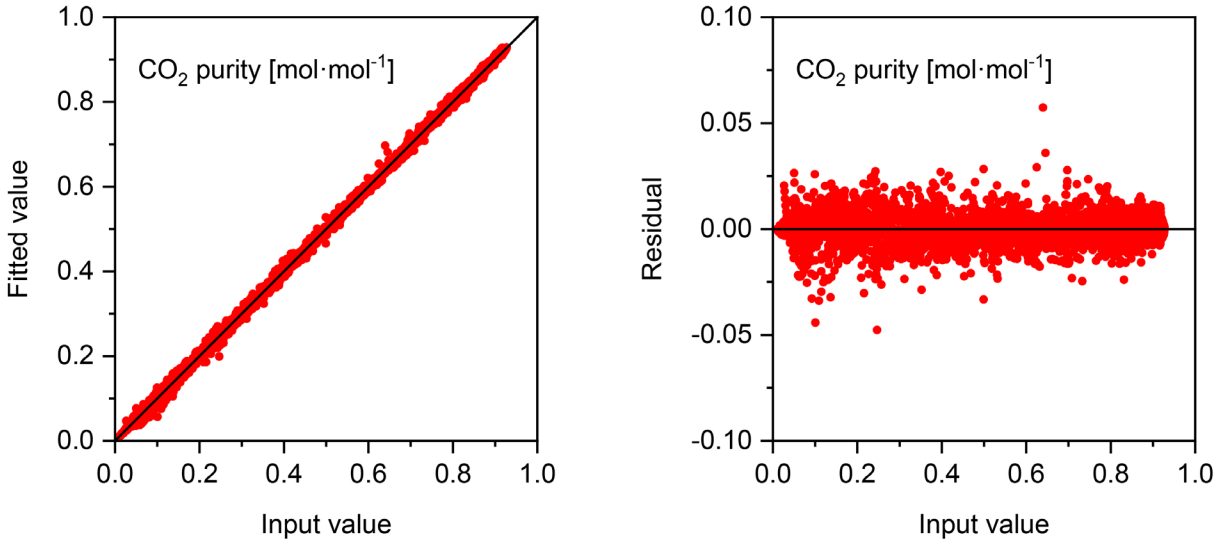

Figure 22 – Parity and residual plots of the surrogate model fit for the CO_2 purity data for the natural gas scenario

Absolute error statistics

Number of points	4992	
Minimum	$6.279 \cdot 10^{-7}$	mol·mol^{-1}
Maximum	$5.731 \cdot 10^{-2}$	
Average	$4.268 \cdot 10^{-3}$	
Median	$2.795 \cdot 10^{-3}$	
Standard deviation	$4.624 \cdot 10^{-3}$	
Margin of error for 99 % confidence interval	$\pm 1.686 \cdot 10^{-4}$	

Percentage error statistics

Percentage error	Number of points greater than	Percentage of total points
5	516	10.3
10	175	3.5
15	75	1.5
20	44	0.9

Recovery

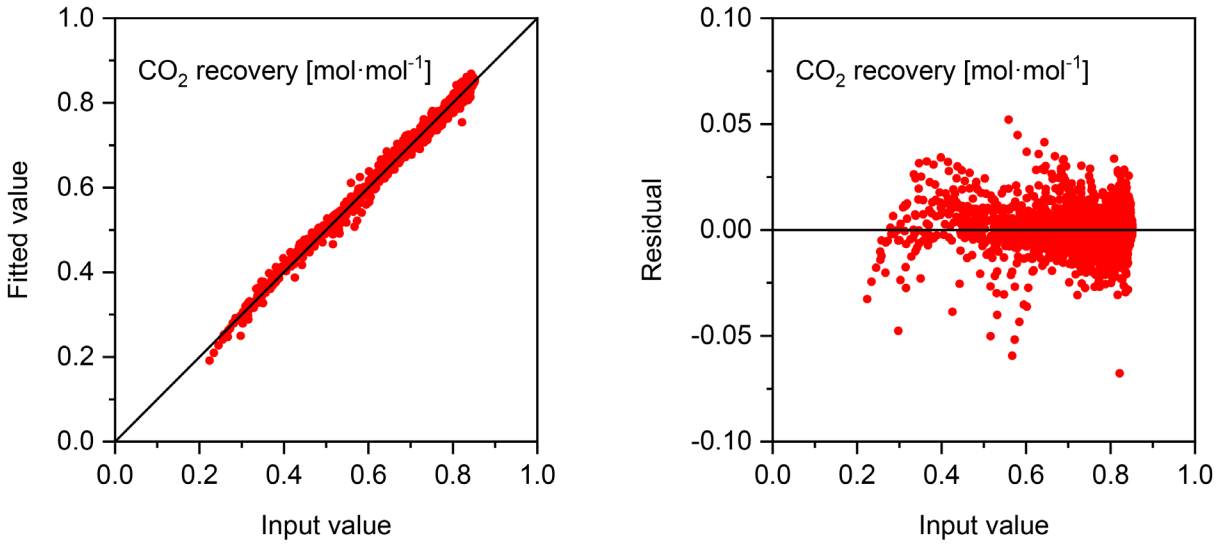

Figure 23 – Parity and residual plots of the surrogate model fit for the CO_2 recovery data for the natural gas scenario

Absolute error statistics

Number of points	4480	
Minimum	$2.499 \cdot 10^{-7}$	mol·mol^{-1}
Maximum	$6.772 \cdot 10^{-2}$	
Average	$3.925 \cdot 10^{-3}$	
Median	$1.508 \cdot 10^{-3}$	
Standard deviation	$5.891 \cdot 10^{-3}$	
Margin of error for 99 % confidence interval	$\pm 2.268 \cdot 10^{-4}$	

Percentage error statistics

Percentage error	Number of points greater than	Percentage of total points
5	46	1.0
10	4	0.1
15	1	0.0
20	0	0.0

Capture cost

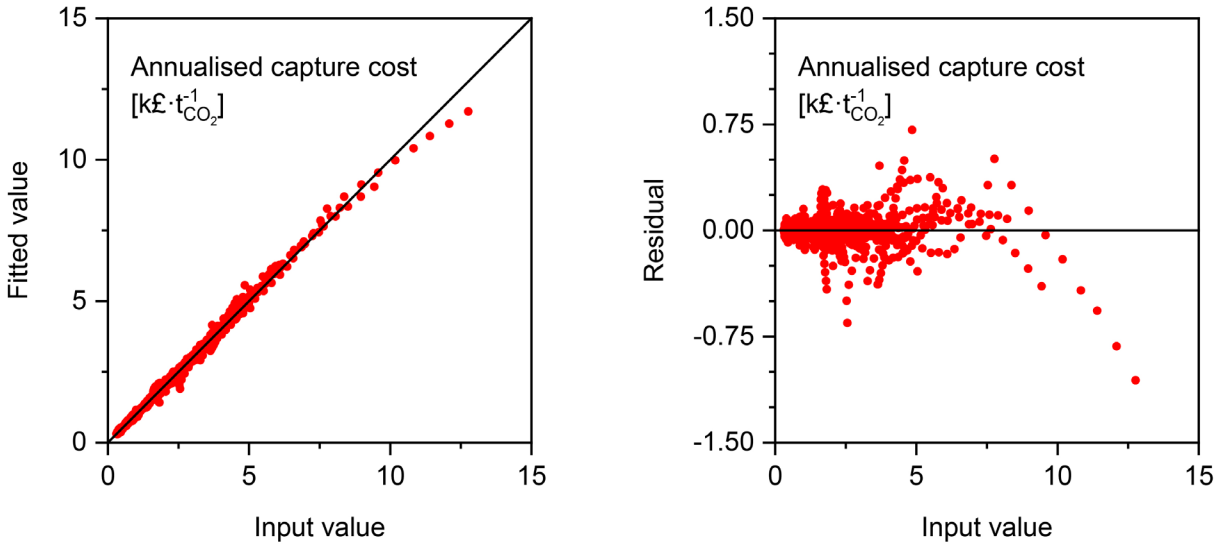

Figure 24 – Parity and residual plots of the surrogate model fit for the CO_2 capture cost data for the natural gas scenario

Absolute error statistics

Number of points	4608	
Minimum	$7.179 \cdot 10^{-7}$	k£·t_{CO2}^{-1}
Maximum	1.059	
Average	$1.791 \cdot 10^{-2}$	
Median	$4.861 \cdot 10^{-3}$	
Standard deviation	$4.821 \cdot 10^{-2}$	
Margin of error for 99 % confidence interval	$\pm 1.830 \cdot 10^{-3}$	

Percentage error statistics

Percentage error	Number of points greater than	Percentage of total points
5	277	6.0
10	58	1.3
15	13	0.3
20	3	0.1

Coal

Purity

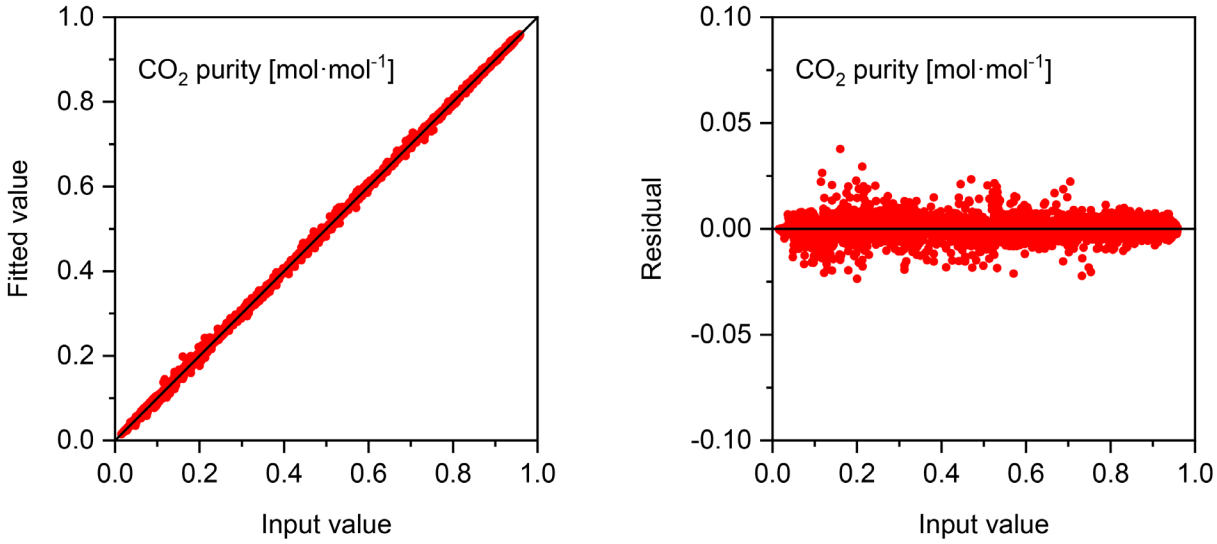

Figure 25 – Parity and residual plots of the surrogate model fit for the CO_2 purity data for the coal scenario

Absolute error statistics

Number of points	4992	
Minimum	$4.911 \cdot 10^{-8}$	mol·mol^{-1}
Maximum	$3.765 \cdot 10^{-2}$	
Average	$2.467 \cdot 10^{-3}$	
Median	$1.461 \cdot 10^{-3}$	
Standard deviation	$3.087 \cdot 10^{-3}$	
Margin of error for 99 % confidence interval	$\pm 1.126 \cdot 10^{-4}$	

Percentage error statistics

Percentage error	Number of points greater than	Percentage of total points
5	192	3.8
10	44	0.9
15	15	0.3
20	5	0.1

Recovery

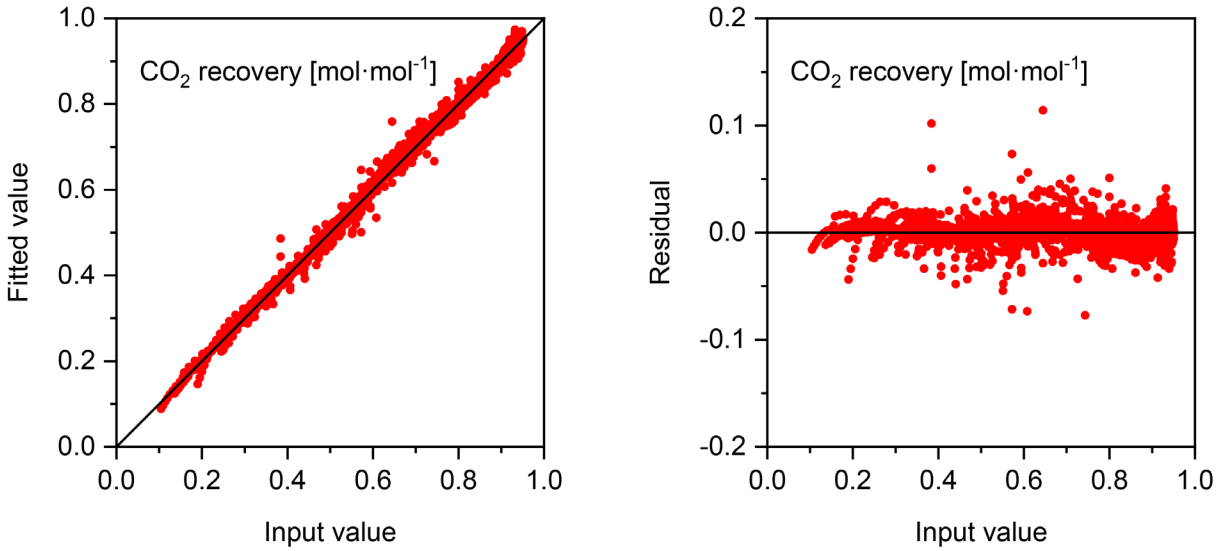

Figure 26 – Parity and residual plots of the surrogate model fit for the CO_2 recovery data for the coal scenario

Absolute error statistics

Number of points	4992	
Minimum	$6.569 \cdot 10^{-8}$	mol·mol^{-1}
Maximum	$1.141 \cdot 10^{-1}$	
Average	$4.038 \cdot 10^{-3}$	
Median	$9.967 \cdot 10^{-4}$	
Standard deviation	$7.201 \cdot 10^{-3}$	
Margin of error for 99 % confidence interval	$\pm 2.626 \cdot 10^{-4}$	

Percentage error statistics

Percentage error	Number of points greater than	Percentage of total points
5	96	1.9
10	15	0.3
15	6	0.1
20	2	0.0

Capture cost

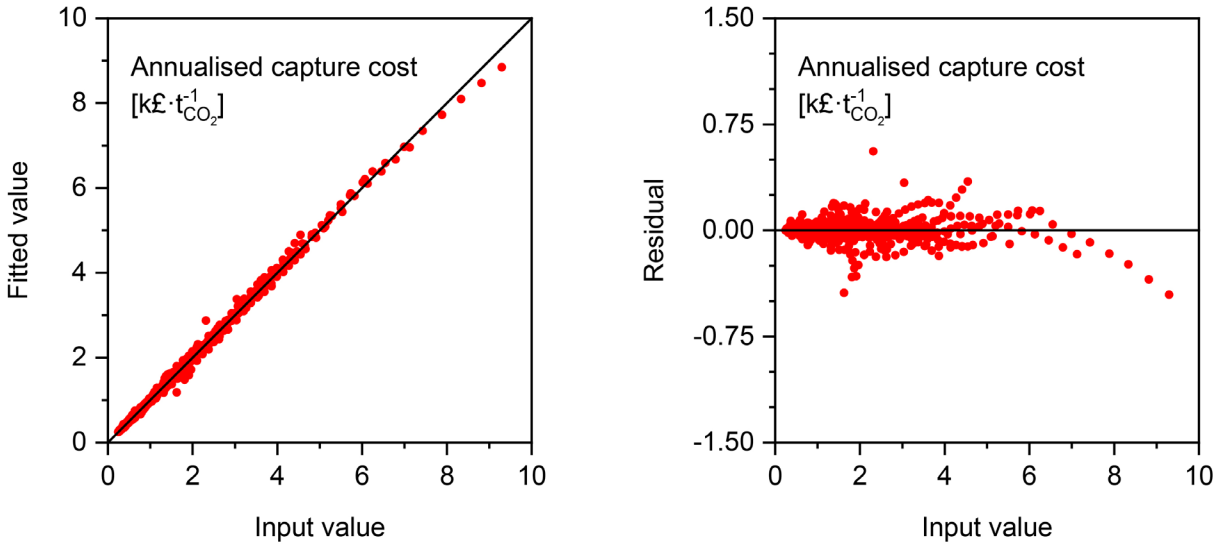

Figure 27 – Parity and residual plots of the surrogate model fit for the CO_2 capture cost data for the coal scenario

Absolute error statistics

Number of points	4992	
Minimum	$9.516 \cdot 10^{-7}$	k£·t_{CO2}^{-1}
Maximum	0.5583	
Average	$9.476 \cdot 10^{-3}$	
Median	$1.381 \cdot 10^{-3}$	
Standard deviation	$2.794 \cdot 10^{-2}$	
Margin of error for 99 % confidence interval	$\pm 1.019 \cdot 10^{-3}$	

Percentage error statistics

Percentage error	Number of points greater than	Percentage of total points
5	134	2.7
10	24	0.5
15	6	0.1
20	2	0.0

Cement

Purity

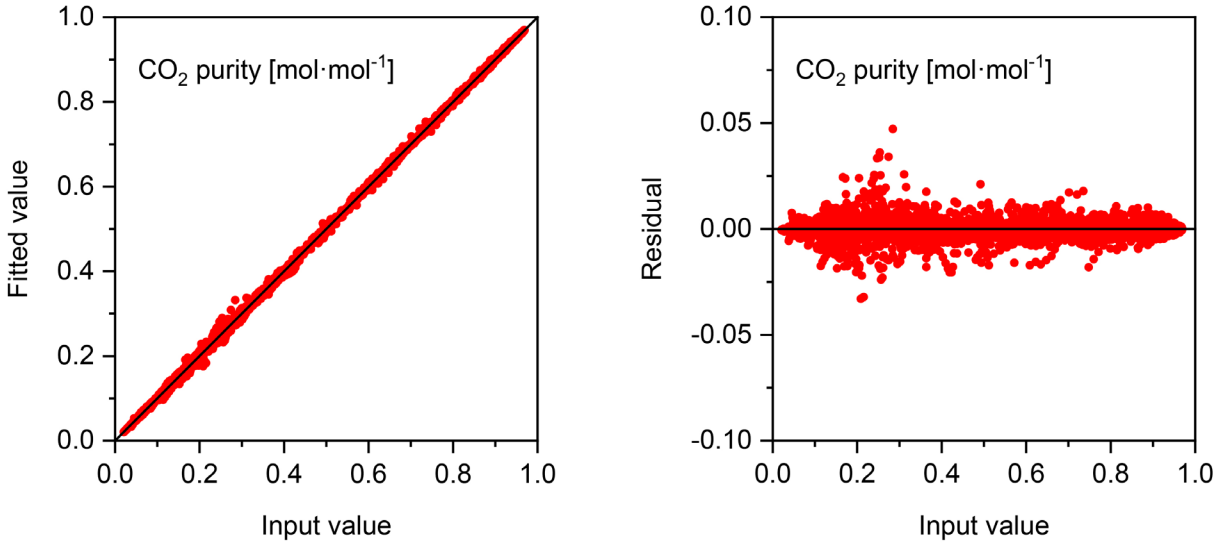

Figure 28 – Parity and residual plots of the surrogate model fit for the CO_2 purity data for the cement scenario

Absolute error statistics

Number of points	4992	
Minimum	$4.574 \cdot 10^{-7}$	mol·mol^{-1}
Maximum	$4.718 \cdot 10^{-2}$	
Average	$2.330 \cdot 10^{-3}$	
Median	$1.203 \cdot 10^{-4}$	
Standard deviation	$3.293 \cdot 10^{-3}$	
Margin of error for 99 % confidence interval	$\pm 1.201 \cdot 10^{-4}$	

Percentage error statistics

Percentage error	Number of points greater than	Percentage of total points
5	146	2.9
10	22	0.4
15	4	0.1
20	0	0.0

Recovery

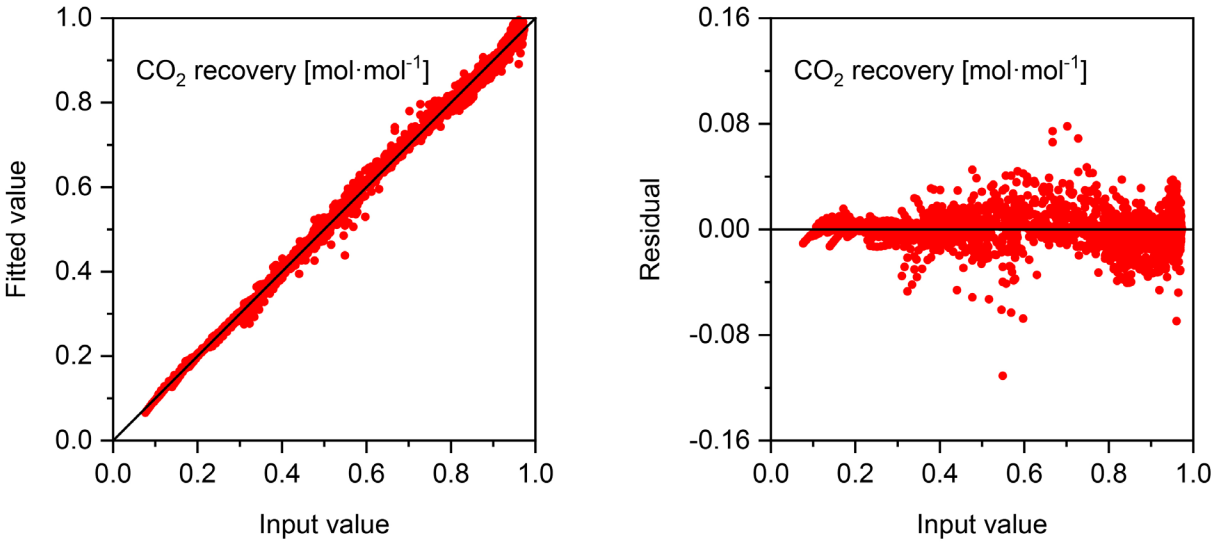

Figure 29 – Parity and residual plots of the surrogate model fit for the CO_2 recovery data for the cement scenario

Absolute error statistics

Number of points	5104	
Minimum	$3.538 \cdot 10^{-7}$	mol·mol^{-1}
Maximum	$1.109 \cdot 10^{-1}$	
Average	$4.519 \cdot 10^{-3}$	
Median	$1.068 \cdot 10^{-6}$	
Standard deviation	$7.776 \cdot 10^{-3}$	
Margin of error for 99 % confidence interval	$\pm 2.805 \cdot 10^{-4}$	

Percentage error statistics

Percentage error	Number of points greater than	Percentage of total points
5	91	1.8
10	15	0.3
15	1	0.0
20	1	0.0

Capture cost

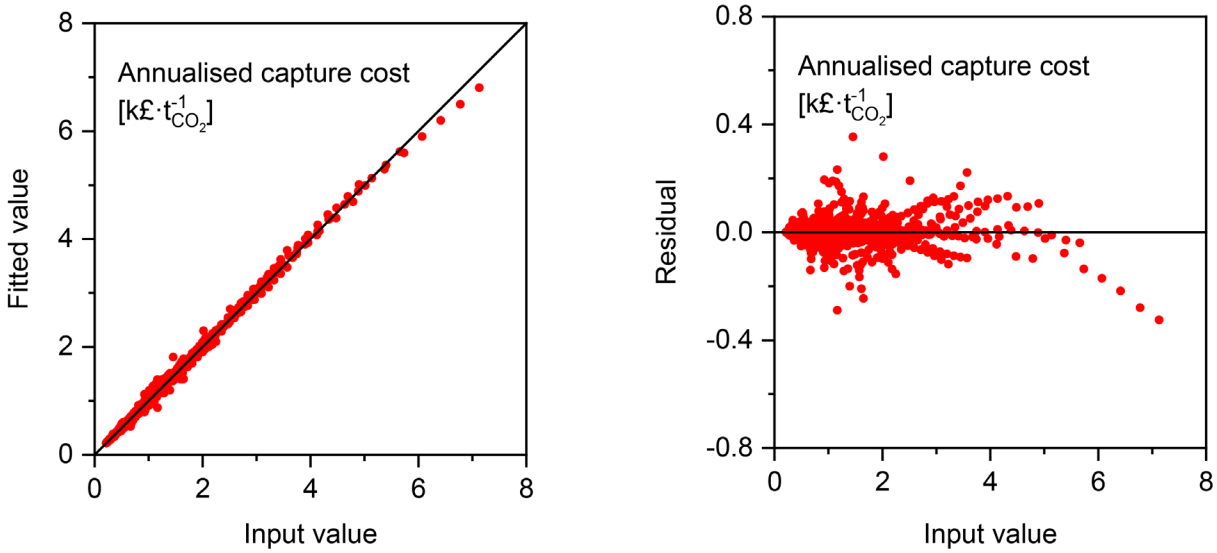

Figure 30 – Parity and residual plots of the surrogate model fit for the CO_2 capture cost data for the cement scenario

Absolute error statistics

Number of points	4992	
Minimum	$4.990 \cdot 10^{-7}$	k£·t_{CO2}^{-1}
Maximum	0.3536	
Average	$8.045 \cdot 10^{-3}$	
Median	$1.297 \cdot 10^{-3}$	
Standard deviation	$2.186 \cdot 10^{-2}$	
Margin of error for 99 % confidence interval	$\pm 7.974 \cdot 10^{-4}$	

Percentage error statistics

Percentage error	Number of points greater than	Percentage of total points
5	148	3.0
10	31	0.6
15	8	0.2
20	4	0.1

Steel

Purity

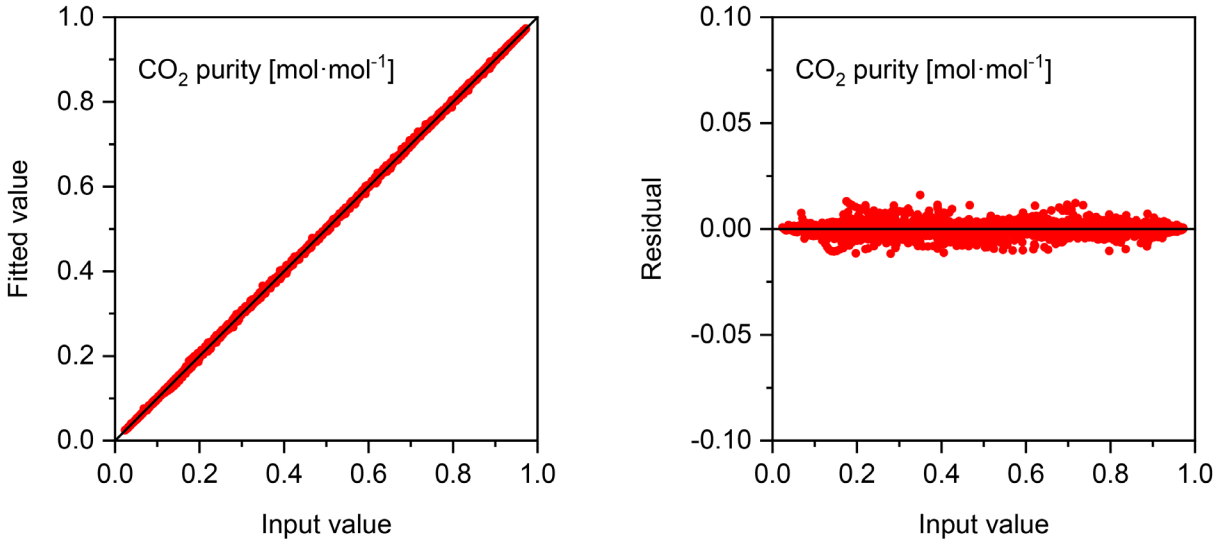

Figure 31 – Parity and residual plots of the surrogate model fit for the CO_2 purity data for the steel scenario

Absolute error statistics

Number of points	5200	
Minimum	$4.327 \cdot 10^{-8}$	mol·mol^{-1}
Maximum	$1.598 \cdot 10^{-2}$	
Average	$1.241 \cdot 10^{-3}$	
Median	$6.914 \cdot 10^{-4}$	
Standard deviation	$1.641 \cdot 10^{-3}$	
Margin of error for 99 % confidence interval	$\pm 5.864 \cdot 10^{-5}$	

Percentage error statistics

Percentage error	Number of points greater than	Percentage of total points
5	18	0.3
10	1	0.0
15	0	0.0
20	0	0.0

Recovery

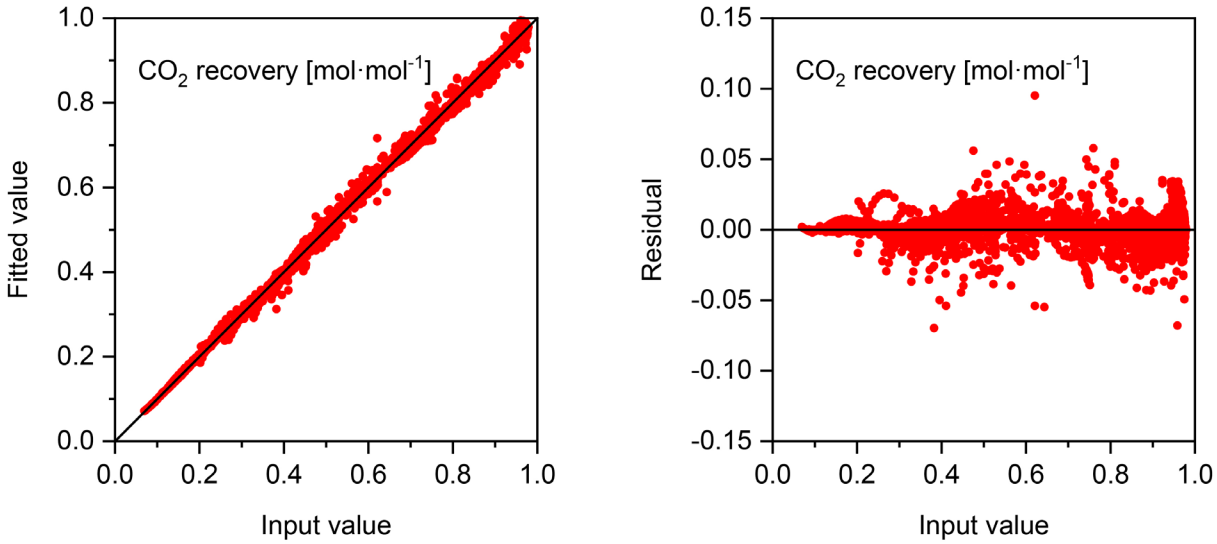

Figure 32 – Parity and residual plots of the surrogate model fit for the CO_2 recovery data for the steel scenario

Absolute error statistics

Number of points	5200	
Minimum	$1.169 \cdot 10^{-9}$	mol·mol^{-1}
Maximum	$9.514 \cdot 10^{-2}$	
Average	$4.000 \cdot 10^{-3}$	
Median	$8.747 \cdot 10^{-4}$	
Standard deviation	$7.143 \cdot 10^{-3}$	
Margin of error for 99 % confidence interval	$\pm 2.552 \cdot 10^{-4}$	

Percentage error statistics

Percentage error	Number of points greater than	Percentage of total points
5	79	1.5
10	7	0.1
15	2	0.0
20	0	0.0

Capture cost

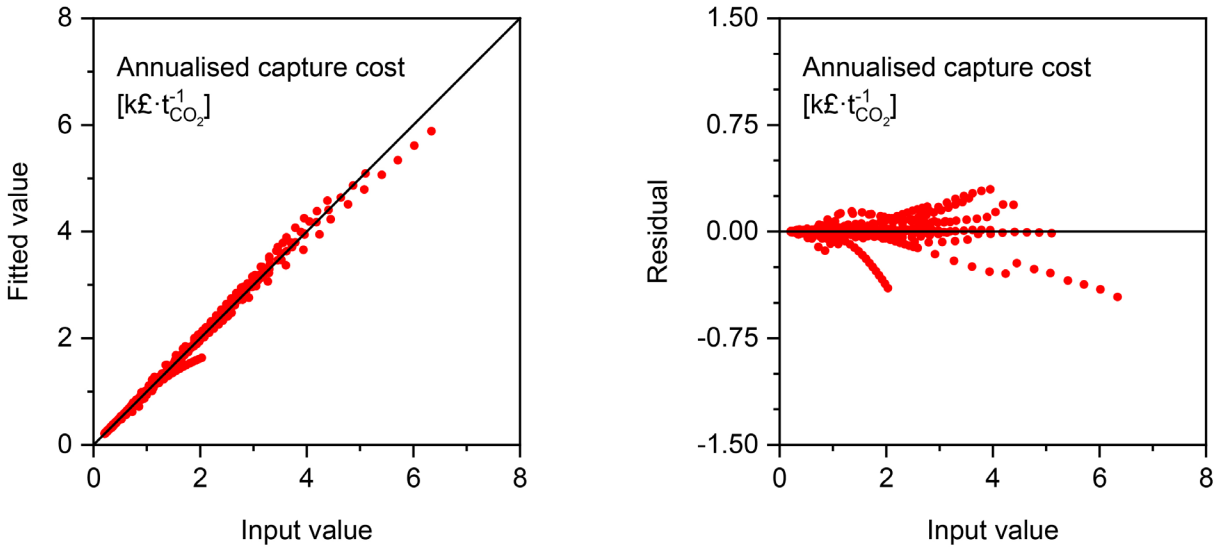

Figure 33 – Parity and residual plots of the surrogate model fit for the CO_2 capture cost data for the steel scenario

Absolute error statistics

Number of points	5200	
Minimum	$5.810 \cdot 10^{-7}$	k£·t_{CO2}^{-1}
Maximum	0.4602	
Average	$5.527 \cdot 10^{-3}$	
Median	$7.742 \cdot 10^{-4}$	
Standard deviation	$2.532 \cdot 10^{-2}$	
Margin of error for 99 % confidence interval	$\pm 9.047 \cdot 10^{-4}$	

Percentage error statistics

Percentage error	Number of points greater than	Percentage of total points
5	69	1.3
10	14	0.3
15	6	0.1
20	0	0.0

Power plant flue-gas determination

A method was devised to determine the flow rate and composition of post-combustion flue gases. This was to allow on-the-fly calculation of the flue-gas stream given a fuel source and a power generation capacity.

The mass flow rate of fuel, m_{fuel}, with lower heating value, LHV_{fuel}, that is required to be combusted in order to produce a given amount of electrical power, P_{elec}, with a given plant round-trip-efficiency, η_{RT}, is given by the equation below.

$$\dot{m}_{fuel} = \frac{P_{elec}}{LHV_{fuel} \cdot \eta_{RT}}$$

This is the basis for this method, and examples for natural gas and coal are given below. The natural gas case is fairly trivial.

Natural-gas

It is assumed that the natural gas is pure methane, however, this method can be adapted for other gaseous fuel compositions.

$P_{elec} = 400$ MW

$LHV_{fuel} = 50\ \text{MJ}\cdot\text{kg}^{-1}$

$\eta_{RT} = 0.55$

$$\dot{m}_{fuel} = \frac{400}{50 \cdot 0.55} = 14.55\ \text{kg}\cdot\text{s}^{-1}$$

$$\dot{n}_{fuel} = \frac{14.55}{16} = 0.9091\ \text{kmol}\cdot\text{s}^{-1}$$

Assuming and air to fuel ratio (AFR) of 43 on a mass basis for an NGCC power plant, and assuming complete combustion of the fuel, a mass balance can be carried out.

$$\dot{m}_{air} = \dot{m}_{fuel} \times AFR$$

$$\dot{n}_{air} = \frac{\dot{m}_{air}}{28.84}$$

$$\dot{n}_{O_2}^{in} = \dot{n}_{air} \times 0.21$$

$$\dot{n}_{N_2}^{in} = \dot{n}_{air} \times 0.79$$

$$CH_4 + 2O_2 \rightleftharpoons CO_2 + 2H_2O$$

Component	In	Reacted	Out
Fuel	0.9091	-0.9091	0.0000
O_2	4.5557	-1.8182	2.7375
N_2	17.138	0.0000	17.138
CO_2	-	+0.9091	0.9091
H_2O	-	+1.8182	1.8182

In this work, as it is assumed that the flue gas is provided dry, so the H_2O is subtracted to give the dry flow rate of flue gas.

Although some excess O_2 is present, it is assumed that the separation taking place is only a CO_2/N_2 separation, however, the O_2 is included in the mass flow rate calculation.

$$y_{CO_2} = \frac{\dot{n}_{CO_2}}{\dot{n}_{CO_2} + \dot{n}_{O_2} + \dot{n}_{N_2}}$$
$$\dot{n}_{fluegas} = \dot{n}_{CO_2} + \dot{n}_{O_2} + \dot{n}_{N_2}$$
$$\dot{m}_{fluegas} = \left[y_{CO_2} \cdot MW_{CO_2} + y_{N_2} \cdot MW_{N_2} + y_{O_2} \cdot MW_{O_2} \right] \cdot \dot{n}_{fluegas}$$

This yields a flue gas composition of 4.37 $\%_{mol}$ CO_2, and a flow rate of 607 $kg \cdot s^{-1}$ for an electrical output power of 400 MW.

Coal

For the coal case the overall procedure is the same, however, additional steps are required to determine the LHV of the coal, and the required air to fuel ratio.

The HHV of the coal sample is determined using the method developed by Majumder *et al.*[1] below, which is based on proximate analysis of a coal sample. Where HHV is the higher heating value in $MJ \cdot kg^{-1}$, A is the mass percentage of ash, M the mass percentage of moisture, V_M the mass percentage of volatile matter, and F_C the mass percentage of fixed carbon; all on an as received basis.

$$HHV = -0.03 \times A - 0.11 \times M + 0.33 \times V_M + 0.35 \times F_C$$

The process will be demonstrated for the high-rank coal used in this work.

Vassilev *et al.*[2] undertook a statistical analysis on a range of low, medium, and high-rank coals, to provide an average representative of each.

The proximate analysis of high-rank coal was 2.6 $\%_{wt}$ moisture, 16.5 $\%_{wt}$ volatile matter, 65.9 $\%_{wt}$ fixed carbon, and 15.0 $\%_{wt}$ ash.

$$\begin{aligned} HHV &= -0.03 \times 15.0 - 0.11 \times 2.6 + 0.33 \times 16.5 + 0.35 \times 65.9 \\ &= 27.774 \text{ MJ} \cdot \text{kg}^{-1} \end{aligned}$$

The ultimate analysis of the coal is then used to determine the 'molecular formula' of the coal sample.

The coal sample consisted 88.7 $\%_{wt}$ carbon, 4.1 $\%_{wt}$ hydrogen, 1.2 $\%_{wt}$ nitrogen, and 1.6 $\%_{wt}$ sulphur on a dry and ash-free basis.

It was assumed that the coal was composed of C, H, and O, such that the combustion produces only CO_2 and H_2O. This results in a composition of 91.0 $\%_{wt}$ carbon, 4.2 $\%_{wt}$ hydrogen, and 4.8 $\%_{wt}$ oxygen. The molecular formula which results in this composition is then determined.

In this case: $C_{25}H_{14}O$, with molar mass 330 $g \cdot mol^{-1}$

The HHV can now be converted to the LHV.

Considering all the H present in the coal will form H_2O:

$$n\left(H_2O\right)_{DAF}^{produced} = \frac{14}{2} \times \frac{1000}{330} = 21.21 \ \frac{mol\left(H_2O\right)}{kg_{DAF}^{coal}}$$

It is now necessary to convert the dry and ash-free basis to the as-received basis:

$$\begin{aligned} n\left(H_2O\right)_{AR}^{produced} &= \frac{n\left(H_2O\right)_{DAF}^{produced}}{1 + \frac{M + A}{100}} = \frac{21.21}{1 + \frac{2.6 + 15.0}{100}} \\ &= 18.0 \ \frac{mol\left(H_2O\right)}{kg_{AR}^{coal}} \end{aligned}$$

The Δh_{lv} of water at 1 atm is 40.65 kJ·mol^{-1}.

$$LHV = HHV - \Delta h_{lv} \cdot n\left(H_2O\right)$$
$$= 27.774 - \frac{40.65 \times 18.0}{1000} = 27.04 \text{ MJ} \cdot \text{kg}^{-1}$$

Using the molecular formula, it is also possible to determine the stoichiometric amount of air required for combustion.

$$C_{25}H_{14}O + 15.5O_2 \rightleftharpoons 12.5CO_2 + 7H_2O$$

The stoichiometric mass of air required for 330 g (1 mole) of high-rank coal is 2362 g, thus the stoichiometric air to fuel ratio is 7.16.

It is assumed the coal is combusted in 25 % excess air, thus the final air to fuel ratio is 8.95, and a value of 9 is used in the model.

With the LHV (27 MJ·kg^{-1}), and AFR (9) determined, it is now possible to carry out the mass balance in the same way as per natural gas.

It is assumed that the coal plant is of the ultra-supercritical (USC) type with a round trip efficiency of 45 %.

The mass balance is shown for a 500 MW plant.

Component	**In**	**Reacted**	**Out**
Fuel	0.1245	-0.1245	0.0000
O_2	2.677	-1.930	0.7468
N_2	10.07	0.000	10.07
CO_2	-	+1.556	1.556
H_2O	0.06094	+0.8716	0.9325

Using the same assumptions as for the natural gas case, this results in a flue gas of 12.5 $\%_{mol}$ CO_2, and a flow rate of 377.1 kg·s^{-1}.

For interest of the reader, using the same procedure for the low-rank coal provided in Vassilev *et al*[2].

LHV = 18.7 MJ·kg^{-1}

AFR = 13
P_{elec} = 500 MW
η_{RT} = 0.40

y_{CO2} = 13.5 $\%_{mol}$ CO_2
Q = 900 $kg \cdot s^{-1}$

Adsorbent input data

This section contains the input data for the adsorbents evaluated including the: dual-site Langmuir isotherm fitting parameters, physical properties, and any data sources.

The numerical isotherm data for adsorbents which required data digitisation is provided as additional supplementary information.

Units are as follows:

m – $mol \cdot kg^{-1}$

b_0 – bar^{-1}

ΔH – $J \cdot mol^{-1}$

ϱ – $kg \cdot m^{-3}$

ε – $m^3 \cdot m^{-3}$

C_P – $J \cdot kg^{-1} \cdot K^{-1}$

	Mg-MOF-74	Ni-MOF-74	HKUST-1	MOF-505
Isotherm parameters				
CO_2				
m_1	6.405	6.459	15.43	2.579
$b_{0,1}$	$1.701 \cdot 10^{-6}$	$1.116 \cdot 10^{-6}$	$5.669 \cdot 10^{-6}$	$7.777 \cdot 10^{-5}$
ΔH_1	42843	40846	28526	25715
m_2	9.802	363.5	-	29.54
$b_{0,2}$	$7.320 \cdot 10^{-6}$	$1.237 \cdot 10^{-4}$	-	$5.835 \cdot 10^{-7}$
ΔH_2	26394	8842.0	-	27369
N_2				
m_1	114.0	7.120	9.014	41.25
$b_{0,1}$	$5.682 \cdot 10^{-6}$	$1.208 \cdot 10^{-5}$	$5.829 \cdot 10^{-5}$	$5.008 \cdot 10^{-6}$
ΔH_1	$5.302 \cdot 10^{-8}$	23540	16039	18093
m_2	5.935	-	-	-
$b_{0,2}$	$1.954 \cdot 10^{-5}$	-	-	-
ΔH_2	22803	-	-	-
Isotherm data source	3	4	5	6
Digitised data	No	Yes	No	Yes

Physical properties				
Density	457	602	446	467
Porosity	0.758	0.757	0.808	0.785
CIF file source	7	8	9	10
Heat capacity	989	781	803	925
Heat capacity source	-	-	-	-

	MOF-505@GO	Mixed ligand Co MOF	MIL-101(Cr)	UTSA-16
Isotherm parameters				
CO_2				
m_1	3.627	1.700	3.589	4.079
$b_{0,1}$	$4.246 \cdot 10^{-4}$	$1.673 \cdot 10^{-6}$	$1.961 \cdot 10^{-6}$	$6.000 \cdot 10^{-6}$
ΔH_1	21632	33810	32356	34250
m_2	40.71	8.456	1.177	1.289
$b_{0,2}$	$5.067 \cdot 10^{-7}$	$2.616 \cdot 10^{-6}$	$7.125 \cdot 10^{-6}$	$1.626 \cdot 10^{-8}$
ΔH_2	27097	26929	25332	37820
N_2				
m_1	41.25	53.96	10.14	1.326
$b_{0,1}$	$5.008 \cdot 10^{-6}$	$2.838 \cdot 10^{-5}$	$2.028 \cdot 10^{-5}$	$2.154 \cdot 10^{-3}$
ΔH_1	18093	12800	2243.8	8558
m_2	-	-	3.072	1.773
$b_{0,2}$	-	-	$5.387 \cdot 10^{-6}$	$1.669 \cdot 10^{-7}$
ΔH_2	-	-	22864	30280
Isotherm data source	6	11	12	13
Digitised data	Yes	Yes	Yes	No

Physical properties				
Density	467	408	208	787
Porosity	0.785	0.725	0.893	0.605
CIF file source	10	11	14	15
Heat capacity	925	916	936	878
Heat capacity source	-	-	-	-

	MOF-177	NiDABCO	CuDABCO	ZnDABCO
Isotherm parameters				
CO_2				
m_1	2841	138.1	211.1	227.6
$b_{0,1}$	$1.359 \cdot 10^{-6}$	$5.860 \cdot 10^{-6}$	$1.632 \cdot 10^{-6}$	$1.752 \cdot 10^{-6}$
ΔH_1	13315	18302	17186	18566
m_2	-	37.61	250.4	269.2
$b_{0,2}$	-	$8.667 \cdot 10^{-7}$	$5.698 \cdot 10^{-7}$	$6.080 \cdot 10^{-7}$
ΔH_2	-	23645	21540	21490
N_2				
m_1	113.6	10.18	7.899	6.442
$b_{0,1}$	$3.854 \cdot 10^{-5}$	$2.175 \cdot 10^{-5}$	$8.179 \cdot 10^{-5}$	$9.811 \cdot 10^{-5}$
ΔH_1	9253.9	17468	13051	14379
m_2	97.73	-	-	-
$b_{0,2}$	$2.354 \cdot 10^{-5}$	-	-	-
ΔH_2	1640.9	-	-	-
Isotherm data source	[3]	[16]	[16]	[17]
Digitised data	No	No	No	No

Physical properties				
Density	306	421	421	334
Porosity	0.883	0.757	0.757	0.840
CIF file source	[18]	[19]	Assumed same as NiDABCO	[20]
Heat capacity	1067	1008	985	1002
Heat capacity source	-	-	-	-

	Zn(BPDC)(BPP)	ZIF-8	ED-ZIF-8	ZIF-68
Isotherm parameters				
CO_2				
m_1	6.855	7.759	28.07	6.082
$b_{0,1}$	$3.966 \cdot 10^{-6}$	$1.152 \cdot 10^{-4}$	$1.006 \cdot 10^{-4}$	$2.140 \cdot 10^{-5}$
ΔH_1	22873	16100	13732	24109
m_2	0.6085	-	1.503	-
$b_{0,2}$	$1.948 \cdot 10^{-5}$	-	$2.640 \cdot 10^{-5}$	-
ΔH_2	28302	-	8757.9	-
N_2				
m_1	0.3702	154.8	327.5	15.71
$b_{0,1}$	$8.652 \cdot 10^{-9}$	$2.164 \cdot 10^{-5}$	$1.189 \cdot 10^{-5}$	$2.041 \cdot 10^{-5}$
ΔH_1	38425	8478.9	8743.1	14780
m_2	-	-	-	-
$b_{0,2}$	-	-	-	-
ΔH_2	-	-	-	-
Isotherm data source	[21]	[22]	[22]	[23]
Digitised data	Yes	Yes	Yes	Yes

Physical properties				
Density	596	405	405	521
Porosity	0.540	0.752	0.752	0.684
CIF file source	[21]	[24]	Assumed same as ZIF-8	[25]
Heat capacity	1088	1058	1058	905
Heat capacity source	-	-	-	-

	ZIF-69	ZIF-70	ZIF-78	ZIF-79
Isotherm parameters				
CO_2				
m_1	5.801	6.984	1.596	1.668
$b_{0,1}$	$2.310 \cdot 10^{-5}$	$9.335 \cdot 10^{-5}$	$3.121 \cdot 10^{-5}$	$5.046 \cdot 10^{-5}$
ΔH_1	24365	19418	29052	25106
m_2	-	-	4.216	4.223
$b_{0,2}$	-	-	$9.512 \cdot 10^{-6}$	$3.453 \cdot 10^{-6}$
ΔH_2	-	-	25543	26144
N_2				
m_1	13.39	2.806	2.399	1.747
$b_{0,1}$	$4.709 \cdot 10^{-5}$	$2.588 \cdot 10^{-4}$	$1.822 \cdot 10^{-4}$	$1.801 \cdot 10^{-4}$
ΔH_1	13418	13061	14904	14854
m_2	-	-	-	-
$b_{0,2}$	-	-	-	-
ΔH_2	-	-	-	-
Isotherm data source	23	23	23	23
Digitised data	Yes	Yes	Yes	Yes

Physical properties				
Density	595	392	558	542
Porosity	0.518	0.746	0.608	0.633
CIF file source	25	25	23	23
Heat capacity	905	998	915	990
Heat capacity source	-	-	-	-

	ZIF-81	ZIF-82	Activated Carbon	Zeolite 5A
Isotherm parameters				
CO_2				
m_1	1.546	1.669	3.234	1.794
$b_{0,1}$	$2.307 \cdot 10^{-5}$	$3.208 \cdot 10^{-5}$	$1.395 \cdot 10^{-5}$	$4.198 \cdot 10^{-5}$
ΔH_1	27493	27436	29302	38748
m_2	13.28	23.56	6.933	1.702
$b_{0,2}$	$6.028 \cdot 10^{-6}$	$8.874 \cdot 10^{-6}$	$7.010 \cdot 10^{-7}$	$1.645 \cdot 10^{-5}$
ΔH_2	22575	21464	15000	35225
N_2				
m_1	2.588	3.236	50.36	36.65
$b_{0,1}$	$1.536 \cdot 10^{-4}$	$2.874 \cdot 10^{-4}$	$5.187 \cdot 10^{-6}$	$3.844 \cdot 10^{-6}$
ΔH_1	14205	12812	16252	19432
m_2	-	-	50.36	36.65
$b_{0,2}$	-	-	$5.187 \cdot 10^{-6}$	$3.844 \cdot 10^{-6}$
ΔH_2	-	-	16252	19432
Isotherm data source	[23]	[23]	[26]	[27]
Digitised data	Yes	Yes	No	No

Physical properties				
Density	656	474	481	747
Porosity	0.633	0.646	0.690	0.517
CIF file source	[23]	[23]	ϱ, ϵ, C_P all from C_P source	ϱ, ϵ, C_P all from C_P source
Heat capacity	811	928	1050	920
Heat capacity source	-	-	[28]	[27]

	Zeolite 13X
Isotherm parameters	
CO_2	
m_1	2.808
$b_{0,1}$	$4.731 \cdot 10^{-5}$
ΔH_1	32194
m_2	2.498
$b_{0,2}$	$3.301 \cdot 10^{-6}$
ΔH_2	32177
N_2	
m_1	2.020
$b_{0,1}$	$2.036 \cdot 10^{-4}$
ΔH_1	14875
m_2	-
$b_{0,2}$	-
ΔH_2	-
Isotherm data source	[29]
Digitised data	No

Physical properties	
Density	750
Porosity	0.710
CIF file source	ϱ, ε, C_P all from C_P source
Heat capacity	920
Heat capacity source	[28]

Sample heat capacity calculation

Example calculation for UTSA-16

Unit cell formula: $Co_3K(C_6H_8O_7)_2$

Heat capacity of metals from Rumble[30]

$C_P(Co) = 24.81\ J \cdot mol^{-1} \cdot K^{-1}$

$C_P(K) = 29.6\ J \cdot mol^{-1} \cdot K^{-1}$

Heat capacity of ligand using method of Goodman *et al.*[31]

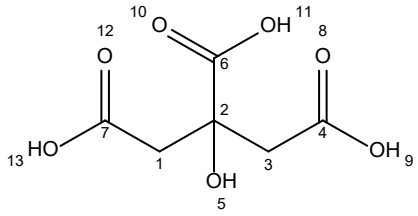

Group	'a' value	Atom numbers	Number of groups
>C<	-0.041	2	1
$>CH_2$	0.1164	1, 3	2
–COOH	0.2102	4, 6, 7	3
–OH	0.1034	5	1

$$A = \exp\left(6.7796 + \sum_k a_k \cdot n_k\right)$$
$$= \exp\left[6.7796 + (-0.041 \times 1) + (0.1164 \times 2) + (0.2102 \times 3) + (0.1034 \times 1)\right]$$
$$= 2221.2\ J \cdot kmol^{-1} \cdot K^{-1}$$

$$C_{P,ligand} = \frac{A}{1000} \times T^{0.79267}$$
$$= \frac{2221.2}{1000} \times (313.15)^{0.79267}$$
$$= 211.302\ J \cdot mol^{-1} \cdot K^{-1}$$

Heat capacity of MOF using method described in paper.

$$
\begin{aligned}
C_{P,MOF} &= \frac{1}{n_{tot}} \sum_k n_k \cdot C_{P,k} \\
&= \frac{1}{6} \cdot \left[\left(3 \times 24.81\right) + \left(1 \times 29.6\right) + \left(2 \times 211.302\right) \right] \\
&= 87.7723 \ \ \mathrm{J \cdot mol^{-1} \cdot K^{-1}}
\end{aligned}
$$

$$
\begin{aligned}
MW_{MOF} &= \frac{1}{n_{tot}} \sum_k n_k \cdot MW_k \\
&= \frac{1}{6} \cdot \left[\left(3 \times 58.933\right) + \left(1 \times 39.098\right) + \left(2 \times 192.123\right) \right] \\
&= 100.024 \ \ \mathrm{g \cdot mol^{-1}}
\end{aligned}
$$

$$
\begin{aligned}
\hat{C}_{P,MOF} &= \frac{C_{P,MOF}}{MW_{MOF}} \times 1000 \\
&= \frac{87.7723}{100.024} \times 1000 \\
&= 877.5 \ \ \mathrm{J \cdot kg^{-1} \cdot K^{-1}}
\end{aligned}
$$

Adsorption model

The adsorption process is a 1-bed, 3-step cycle, and modelled based on the work by Maring and Webley[28]. The model was implemented as described in their work, with the exception that 500 discretised steps were used for the desorption and adsorption step calculations instead of the specified 100 in the paper.

Two additional parameters were also included in the desorption step loop.

The first is to determine the actual volume of gas removed by vacuum, using the ideal gas law. Where Δn_k is the moles of gas removed in the k^{th} step, and T_k and P_k are the temperature and pressure of the k^{th} step respectively.

$$V_{vac}^{cycle} = \sum_k \frac{\Delta n_k \cdot R \cdot T_k}{P_k}$$

The second is to determine the total moles of gas removed under vacuum.

$$n_{vac}^{cycle} = \sum_k \Delta n_k$$

Using the outputs from the PVSA model, the process design and economics are then calculated. The process equipment that are sized and costed are shown in the figure below; the equipment is enumerated/parallelised as required.

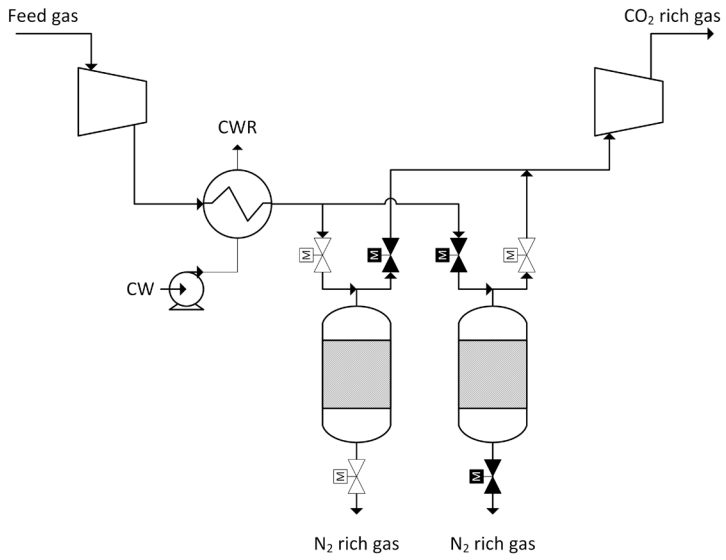

Figure 34 – Process equipment considered for design and costing in the adsorption model

Equipment sizing

Feed compression

The PVSA model returns the blower energy (E_{blower}) required for one cycle, along with the total feed (n_{feed}^{cycle}) for that cycle. The total feed compression shaft work can then be determined given the total feed flow rate (n_{feed}^{total}).

$$W_{comp}^{total} = \frac{E_{blower}}{n_{feed}^{cycle}} \times \dot{n}_{feed}^{total}$$

The total feed volumetric flow rate (in $m^3 \cdot hr^{-1}$) is used to determine the number of compressors, with sizes limited to 10^6 $m^3 \cdot hr^{-1}$ assuming an axial-flow centrifugal type.

$$N_{comp} = \left\lceil \frac{\dot{m}_{feed}^{total}}{\rho_{T_{feed},P_{feed}}^{gas} \times 10^6} \right\rceil$$

$$W_{comp}^{each} = \frac{W_{comp}^{total}}{N_{comp}}$$

Post-compression heat exchanger

The PVSA model returns the temperature of the feed gas post-compression (T_{PC}), assuming an isentropic compression process. Using this temperature, and the user specified adsorption temperature (T_{ads}) the heat exchanger duty can be determined.

$$q_{PC} = \dot{m}_{feed} \times C_P^{feed} \times \left(T_{PC} - T_{ads}\right)$$

If $T_{ads} < T_{PC}$

Cooling water inlet temperature (T_{CW}^{in}): 298.15 K

Cooling water outlet temperature (T_{CW}^{out}): 323.15 K

Overall heat transfer coefficient (U_{CW}): 20 $W \cdot m^{-2} \cdot K^{-1}$

$$\Delta T_{LM} = \frac{\left(T_{ads} - T_{CW}^{in}\right) - \left(T_{PC} - T_{CW}^{out}\right)}{\ln\left(\frac{T_{ads} - T_{CW}^{in}}{T_{PC} - T_{CW}^{out}}\right)}$$

$$A_{PC}^{total} = \frac{q_{PC}}{U_{CW} \cdot \Delta T_{LM}}$$

$$\dot{m}_{CW} = \frac{q_{PC}}{\left(T_{CW}^{out} - T_{CW}^{in}\right) \cdot C_P^{water}}$$

If $T_{ads} > T_{PC}$

To have flexibility in the input range in this work, high-pressure steam (25 bar_a) was used. However, this should be adjusted for each application.

Steam temperature (T_{HPS}): 497.10 K

Enthalpy of vapourisation (ΔH_{vl}): 1840 $kJ \cdot kg^{-1}$

Overall heat transfer coefficient (U_{HPS}): 30 $W \cdot m^{-2} \cdot K^{-1}$

$$\Delta T_{LM} = \frac{\left(T_{ads} - T_{HPS}\right) - \left(T_{PC} - T_{HPS}\right)}{\ln\left(\frac{T_{ads} - T_{HPS}}{T_{PC} - T_{HPS}}\right)}$$

$$A_{PC}^{total} = \frac{q_{PC}}{U_{HPS} \cdot \Delta T_{LM}}$$

$$\dot{m}_{HPS} = \frac{-q_{PC}}{\Delta H_{vl}}$$

The heat exchangers were assumed to be of the shell & tube type, with areas limited to 1000 m^2. This was then used to determine the number of heat exchangers required.

$$N_{PCHX} = \left\lceil \frac{A_{PC}^{total}}{1000} \right\rceil$$

$$A_{PC}^{each} = \frac{A_{PC}^{total}}{N_{PCHX}}$$

Vacuum pumps

The vacuum pumps were enumerated based on manufacturer pump curves. A Pfeiffer Okta 4000 was used between desorption pressures of 0.10 bar_a and 1.00 bar_a, while a Pfeiffer Okta 18000 was used for desorption pressure ≤ 0.10 bara.

The pump curves[32,33] were digitised in order to enable interpolation at any desorption pressure and converted to a piecewise function.

$$x = \log_{10}\left(P \times 1000\right)$$

$$y(x) = \begin{cases} -4.656 \cdot x^4 - 7.2038 \cdot x^3 - 11.8 \cdot x^2 + 1.9683 & -1.79 \le x < -0.71 \\ -0.01265 \cdot x + 4.1590 & -0.71 \le x \le 0.29 \\ 0.2322 \cdot x^2 - 0.9236 \cdot x + 4.4121 & 0.29 < x \le 2 \\ 0.073363 \cdot x^2 - 0.42998 \cdot x + 3.6449 & 2 < x \le 3 \end{cases}$$

$$\dot{V}_{vacpump} = 10^y$$

Where P is the desorption pressure in bar_a, and V_{vac} is the volumetric flow rate in $m^3 \cdot hr^{-1}$. The number of vacuum pumps can then be determined.

First, the total amount of vacuum required per cycle must be determined, and the time available for it to take place. The values used in this work are presented, however, they can be adjusted for a specific case.

Cycles per day (CPD): 24

Adsorption time fraction (ATF): 0.75

This results in a 1-hour cycle time (t_{cycle}), of which 15 minutes is desorption time (t_{vac}).

$$t_{cycle} = \frac{24}{CPD}$$

$$t_{vac} = t_{cycle} \times \left(1 - ATF\right)$$

$$N_{vac} = \left\lceil \frac{V_{vac}^{cycle}}{\dot{V}_{vacpump} \times t_{vac}} \right\rceil$$

The PVSA model does also return the vacuum energy required for a cycle, based on the isentropic compression formulae. However, the power requirements of the vacuum pumps are specified by the manufacturer, so they are used directly. In cases where they are not available, the same method applied for the feed compressors can be used.

Adsorbent beds

Due to the calculation method used in PVSA model regarding the mass of adsorbent and the reported output values, the scaling approach required is atypical.

$$TPDc_{CO_2} = \dot{n}_{feed} \times y_{CO_2}^{feed} \times \mathrm{Rec}_{CO_2} \times \frac{MW_{CO_2}}{10^6}$$

$$n_{CO_2}^{cycle} = \frac{TPDc_{CO_2} \times 10^6}{MW_{CO_2} \times CPD}$$

$$m_{ads} = \frac{n_{CO_2}^{cycle}}{WC_{CO_2} \times 1000}$$

Where $TPDc_{CO2}$ is the tonnes of CO_2 captured per day.

Where n_{feed} is the molar flow rate of the feed is in $mol \cdot day^{-1}$.

Where y_{CO2}^{feed} is molar fraction of CO_2 in the feed gas.

Where Rec_{CO2} is the recovery of CO_2 on a molar basis, returned by the PVSA model.

Where MW_{CO2} is the molar mass of CO_2 in $g \cdot mol^{-1}$.

Where n_{CO2}^{cycle} is the amount of CO_2 captured per cycle in moles.

Where m_{ads} is the mass of adsorbent in tonnes.

Where WC_{CO2} is the working capacity of CO_2 for the adsorbent, returned by the PVSA model.

The sizing of the adsorbent vessels is based on the procedure described in the GPSA Databook[34].

The first step is to calculate the gas velocity that results in the desired pressure drop per unit length of bed, using their modified Ergun equation.

$\Delta P/z$ = 0.3 $psi \cdot ft^{-1}$, recommended maximum is 0.33 $psi \cdot ft^{-1}$.

ΔP_{tot} = 5.8 psi, recommended range is 4 to 8 psi.

The modified Ergun equation parameters for 1/16" extrudates are: x_1 = 0.238, x_2 = 0.0002100.

$$x_2 \cdot \rho_{T_{ads},P_{ads}}^{gas} \cdot V_{gs}^2 + x_1 \cdot \mu \cdot V_{gs}^2 = \frac{\Delta P}{z}$$

Where ϱ is the gas density fed to the column, required to be in $lb \cdot ft^{-3}$.
Where μ is the gas viscosity fed to the column, required to be in cP.
Where V_{gs} is the superficial gas velocity through the bed, in $ft \cdot min^{-1}$.

The quadratic equation can then be solved to obtain the gas velocity.

The length of the bed (in feet) can be determined simply by:

$$L_{bed} = \frac{\Delta P_{tot}}{\Delta P / z}$$

The diameter (in feet) of the bed can be determined by assuming a vessel aspect ratio. For axial flow packed-bed adsorption vessels, this is commonly 1 – and that was used for this work.

$$D_{bed} = \frac{L_{bed}}{AR}$$

As the superficial gas velocity and bed diameter are known, the number of vessels required to achieve this velocity are determined.

The flow rate ($ft^3 \cdot min^{-1}$) that can be put through one bed at the allowable superficial velocity is given by:

$$Q_{bed} = \pi \frac{D_{bed}^2}{4} \cdot V_{gs}$$

The minimum number of beds required can then be calculated:

$$N_{beds}^{\min} = \left\lceil \frac{\dot{m}_{feed}^{total}}{\rho_{T_{ads},P_{ads}}^{gas} \times Q_{bed}} \right\rceil$$

Ensuring that the units are appropriately matched.

The number of beds required from an adsorbent mass basis is also determined:

$$V_{bed} = \pi \frac{D_{bed}^2}{4} \cdot L_{bed}$$

$$m_{ads}^{bed} = V_{bed} \times \rho_{bed}$$

$$N_{beds}^{ads} = \left\lceil \frac{m_{ads}}{m_{ads}^{bed}} \right\rceil$$

The number of beds is then selected:

$$N_{beds} = \max\left\{ N_{beds}^{\min}, N_{beds}^{ads} \right\}$$

This ensures that there is always the requisite number of beds to not exceed the gas velocity.

The actual volumetric flow rate and pressure drop must now be determined and checked to confirm it is still within limits.

$$Q_{bed}^{act} = \left\lceil \frac{\dot{m}_{feed}^{total}}{\rho_{T_{ads},P_{ads}}^{gas} \times N_{beds}} \right\rceil$$

$$V_{gs}^{act} = \frac{4 \cdot Q_{bed}^{act}}{\pi D_{bed}^2}$$

The length of the mass transfer zone (in feet), L_{MTZ}, can now be determined, the constant for 1/16" extrudates is 0.85. Ensure that V_{gs}^{act} is in ft·min^{-1}.

$$L_{MTZ} = \left(\frac{V_{gs}^{act}}{35} \right)^{0.3} \times 0.85$$

$$\Delta P^{act} = \left[x_2 \cdot \rho_{T_{ads},P_{ads}}^{gas} \cdot \left(V_{gs}^{act} \right)^2 + x_1 \cdot \mu \cdot \left(V_{gs}^{act} \right)^2 \right] \times \left(L_{bed} + L_{MTZ} \right)$$

The units are as per the modified Ergun equation above.

The pressure drop should be checked against the recommended ranges, and the outlet pressure.

$$4 \le \Delta P^{act} \le 8\,\text{psi}$$
$$P^{out} = P^{ads} - \Delta P^{act}$$

If the pressure drop is outside the range, then the initial values for pressure drop per unit length, and total pressure drop should be adjusted. If the outlet pressure is below a defined threshold, either the adsorption pressure should be increased, or the initial total pressure drop adjusted.

The number of beds required for capital costing also needs to include the standby beds which are undergoing desorption, so that the total feed flow rate is always accommodated. To account for this, an empirical relationship, the bed multiplication factor (BMF) was developed for this cycle as a function of adsorption time fraction (ATF).

$$BMF = \frac{9.242 \cdot ATF^{-0.986}}{10}$$
$$N_{beds}^{CapEx} = \lceil N_{beds} \times BMF \rceil$$

The vessels are costed on the basis of mass of steel required. The final dimensions are now calculated and the mass per vessel determined.

It is assumed that an additional 3' is being provided for gas distributors and bed supports, and a further 3' is being provided for top and bottom bed support media.

$$L_{T-T} = L_{bed} + L_{MTZ} + 3 + 3$$

The vessel thickness is determined based on AS1210[35]; both the pressure and vacuum thicknesses are calculated, and the greater one chosen. AS1210 uses units of mm for length dimensions, and MPa for pressure, stress, and yield strength values.

$$t_{press}^{circ} = \frac{P \cdot D}{2 \cdot f \cdot \eta - P}$$
$$t_{press}^{long} = \frac{P \cdot D}{4 \cdot f \cdot \eta - P}$$
$$t_{press} = \max\left\{t_{press}^{circ}, t_{press}^{long}\right\}$$

Where P is the design pressure in MPa_g, D the inside diameter in mm, f the yield strength of the material in MPa, and η the weld efficiency.

The design pressure is 10 % above the operating pressure. The yield strength used in this work was 133 MPa (PT460 steel, valid up to 40 mm thickness and 325 °C), and the weld efficiency was assumed to be 1 (which has associated welding and inspection implications).

The thickness that satisfies combined loading requirements is now calculated, with t_{press} being the initial value. This is a check to confirm whether the thickness will also withstand the mass of the vessel and its contents, in addition to the pressure requirements. Accounting for factors such as earthquakes and wind loading/bending moment also takes place here, however, we have excluded those factors.

The mass of the empty vessel is first determined using the correlation in the GPSA Databook[34].

$$m_{shell} = 155 \times \left(t + 0.125\right) \times \left(L + 0.75 \cdot D\right) \cdot D$$

Where t is the vessel thickness in inches, L the tan-tan vessel length in feet, and D the vessel inside diameter in feet; giving the mass of the shell (m_{shell}) in pounds.

The vessel total mass must then be compared for two cases, the operating case, and the hydrostatic test case, with the maximum selected.

$$m_{total}^{op} = m_{shell} + m_{ads}^{bed}$$
$$m_{total}^{hydro} = m_{shell} + V_{vessel} \cdot \rho_{H_2O}$$
$$m_{total} = \max\left\{m_{total}^{op}, m_{total}^{hydro}\right\}$$

All masses are in kg.

The mean diameter (D_m) is calculated, in millimetres.

$$D_m = D + \frac{t}{2}$$

The three principal stresses are then calculated to evaluate against the Tresca criterion.

$$S_b = \frac{4 \times M}{\pi \cdot D_m^2 \cdot t \cdot \cos(\alpha)}$$

$$S_c = \frac{P \cdot D_m}{2 \cdot t \cdot \cos(\alpha)}$$

$$S_w = \frac{-m_{total} \times 9.81}{\pi \cdot D_m \cdot t \cdot \cos(\alpha)}$$

S_b is the bending stress and as mentioned earlier was excluded from this analysis, therefore S_b = 0; α is the half-apex angle for conical sections, so is 0 for cylindrical shells.

$$T = \begin{bmatrix} |S_c| \\ \left|\frac{S_c}{2} + S_w + S_b\right| \\ \left|\frac{S_c}{2} + S_w - S_b\right| \\ \left|S_w + S_b - \frac{S_c}{2}\right| \\ \left|S_w - S_b - \frac{S_c}{2}\right| \end{bmatrix}$$

$$S_E = \max(T)$$

Where S_E is the equivalent stress, in MPa.

The Tresca criterion is satisfied when:

$$S_E \leq \eta \cdot f$$

The minimum allowable thickness is obtained when:

$$S_E = \eta \cdot f$$

In this work, a 10 MPa margin was applied to give the following objective function:

$$\eta \cdot f - S_E(t) - 10 = 0$$

The system (from m_{shell} to this point) can now be solved iteratively to satisfy this criteria.

The solution that satisfies the combined loading objective function for the pressure scenario is:

$$t_{press}^{CL}$$

The thickness required to satisfy the vacuum conditions is then calculated.

$$Z = \frac{\pi \cdot D}{2 \cdot L}$$

$$n^{calc} = Z \cdot \sqrt{\frac{L}{\sqrt{D \cdot t} - 1}}$$

$$n = \begin{cases} 2 & n^{calc} < 2 \\ n^{calc} & \text{otherwise} \end{cases}$$

$$A_a = \frac{1}{n^2 - 1 + \frac{Z^2}{2}} \times \left[\frac{Z^2}{n^2 + Z^2} + t^2 \frac{\left(n^2 - 1 + Z^2\right)^2}{2.73 \times D^2} \right]$$

$$P_e = \frac{2 \cdot E \cdot A_a \cdot t}{D}$$

$$P_y = \frac{2 \cdot 1.5 \cdot f \cdot t}{D}$$

$$P_{calc} = \begin{cases} \frac{P_y \cdot \left(2 - \frac{P_y}{P_e}\right)}{3} & P_e > P_y \\ \frac{P_e}{3} & \text{otherwise} \end{cases}$$

Where E is the Young's modulus of the material, a value of $201 \cdot 10^3$ MPa was used for this work.

An objective function can then be defined:

$$P_{calc}(t) - P_{ext} = 0$$

P_{ext} is the external pressure the vessel experiences in MPa, most easily defined for this work by:

$$P_{ext} = \frac{1.01325 - P_{des}}{10}$$

Where P_{des} is the desorption pressure in bar_a.

The solution of the function will give t_{vac}, the thickness required to withstand the vacuum conditions, and becomes the initial value for the combined loading calculations. The procedure is the same as that for the pressure scenario with the following difference.

$$S_c = \frac{-P_{ext} \cdot D_m}{2 \cdot t \cdot \cos(\alpha)}$$

The solution that satisfies the combined loading objective function for the vacuum case is:

$$t_{vac}^{CL}$$

The vessel thickness can then be obtained:

$$t_{shell} = \max\left\{t_{press}^{CL}, t_{vac}^{CL}\right\}$$

Using the GPSA shell mass equation above, the mass of the vessel can now be calculated using t_{shell} and used for capital cost estimation.

Cost estimation

Once the number of equipment items is determined, and the corresponding cost metric, cost estimation can then take place. An example is provided for one unit, with the data provided for the others.

The IChemE, or factorial cost estimation is used[36,37], with capital costing data obtained from either Peters and Timmerhaus[38,39] (P&T), or Garrett[40], and are indicated respectively. Any specific differences are highlighted. In general, data is obtained and fit to a function to enable interpolation in the model.

- The CEPCI for costs from P&T is 390.4 (CE_{PT})
- The CEPCI for costs from Garret is 320 (CE_{G}).
- The CEPCI used for the current cost is 616.3 (October 2018) (CE_{PV}).
- An exchange rate of 0.76 £·USD^{-1} was used to convert the current day cost to GBP (ER_{PV}).

The IChemE installation cost factors are a function of equipment purchase cost and reported at a different time. Therefore, they have their respective CEPCI and exchange rate values. The updated installation cost factors from January 2000 are used[37].

- The CEPCI for the IChemE installation cost factors is 394.1 (January 2000) (CE_{ICF}).
- An exchange range of 0.61 £·USD^{-1} was used to convert the January 2000 cost in USD to GBP (ER_{ICF}).

The installation cost factors are presented in Table 2 of Brennan[37] and are categorised by type, i.e. installation, piping, instrumentation etc. Each section is treated as a matrix (n × 7) in the model for which the row is specified by the user, and the column is selected based on the equipment purchase cost. The reader is directed to the reference for what each row represents.

For example, if "average bore piping with complex system" were desired for an equipment item with purchase cost £30,000, that would be represented by position (5,4) of the piping factor matrix, resulting in a value of 0.78.

The rows that were selected for each equipment item are represented in a table in their corresponding section and are abbreviated as follows. A value of 0 indicates that that factor was not applied.

- Installation of equipment item = ICF
- Piping including installation = PCF
- Instrumentation = CCF
- Electrical = ECF
- Civil = FCF
- Structures and buildings = BCF
- Lagging = LCF

Feed compression

From the equipment sizing the number of compressors is known, and the shaft work per compressor is also known.

The equipment purchase cost (C_{eqpt}) is first calculated, where W_S is the shaft work of the compressor in kW. Costs are from P&T for a centrifugal type that is motor driven.

$$C_{eqpt} = \exp\left(6.77684\right) \times W_S^{0.9435}$$

The cost in GBP on a January 2000 basis is then determined to enable lookup in the installation cost factor table.

$$C_{ICF} = \frac{C_{eqpt}}{CE_{PT}} \times CE_{ICF} \times ER_{ICF}$$

The rows of the cost factor table used are:

ICF	PCF	CCF	ECF	FCF	BCF	LCF
3	6	4	4	2	3	0

The total installed cost on a present value basis is then given by:

$$C_{ins} = C_{eqpt} \times \left(1 + \sum CF\right)$$

$$C_{total} = C_{ins} \times N_{comp} \times \frac{CE_{PV}}{CE_{PT}} \times ER_{PV}$$

Where ΣCF represents the sum of the cost factors read from the table, and C_{total} is the total installed cost in GBP.

Post-compression heat exchanger

The data for the post-compression heat exchanger is below. Costing data is from P&T.

$$C_{eqpt} = \exp\left(6.152479\right) \times A^{0.713806}$$

Where A is the area of the heat exchanger in m^2. For a floating head shell & tube type, carbon steel shell & tubes, up to 100 psi_g shell side.

ICF	PCF	CCF	ECF	FCF	BCF	LCF
2	6	3	1	1	2	2

Cooling water pump

For this work it was determined that 1 pump capable of providing the flow rate required was available. However, the number of pumps required should be adjusted or calculated accordingly for the reader's application. In this work, 2 pumps were costed as it is customary to have 1 on standby, or operate both cyclically, or operate both at 50 % capacity.

The pump cost curve is based on the parameter $Q \cdot \Delta P$ in $m^3 \cdot s^{-1} \cdot kPa$. It was assumed that 50 kPa pressure loss was required to be overcome in the system.

$$Q_{CW} = \frac{\dot{m}_{CW}}{\rho_{CW}}$$

Costing is from P&T for a horizontal, centrifugal pump including electric motor, with a maximum outlet pressure of 150 psi.

$$C_{eqpt} = \exp\left(9.102953\right) \times \exp\left(0.0122735 \times Q_{CW} \cdot \Delta P_{CW}\right)$$

ICF	PCF	CCF	ECF	FCF	BCF	LCF
1	5	3	4	1	2	0

Adsorbent columns

Costing is from P&T, for carbon steel column shells, where m is the mass of the column in kg.

$$C_{eqpt} = \exp\left(5.483027\right) \times m^{0.615815}$$

ICF	PCF	CCF	ECF	FCF	BCF	LCF
3	4	3	1	1	2	0

Ensure to use N_{beds}^{CapEx} for the number of columns in the total cost calculation.

Adsorbent

The purchase cost of the adsorbent is given by:

$$C_{ads}^{purchase} = C_{ads} \times m_{ads}^{bed} \times N_{beds}^{CapEx}$$

Where C_{ads} is the purchase price for 1 kg of adsorbent, assumed to be 1.5 £·kg^{-1} in this work.

The current day price is converted to the historical cost in order to look up the cost factor table.

$$C_{ads}^{historial} = C_{ads}^{purchase} \times \frac{CE_{PV}}{CE_{ICF}}$$

ICF	PCF	CCF	ECF	FCF	BCF	LCF
4	0	0	0	0	0	0

As the cost of adsorbent is already the present-day value, the installed cost of adsorbent is given only by:

$$C_{total} = C_{ads}^{purchase} \times \left(1 + \sum CF\right)$$

Vacuum pumps

Cost data or curves for vacuum equipment is not readily available. This following cost correlation was available in Garrett. Ensure to use CE_G for present day cost conversion.

$$C_{eqpt} = \exp(11.23543) \times VF^{0.750473}$$

Where VF is the vacuum factor (called capacity factor, CF, in the reference). The factor is lb(air)·hr^{-1}·mmHg^{-1}, the equivalent air mass flow in pounds per hour, at the desired vacuum pressure.

$$\dot{n}_{vac} = \frac{n_{vac}^{cycle}}{n_{feed}^{cycle}} \cdot \dot{n}_{feed}^{total} \times 3600$$

Where n_{vac} is the moles of gas removed under vacuum per hour, n_{vac}^{cycle} is the number of moles of gas removed under vacuum per cycle, n_{feed}^{cycle} is the total moles fed per cycle, where n_{feed}^{total} is the feed gas flow rate in mol·s^{-1}.

The air equivalent mass (M_{AE}) can then be determined, in pounds.

$$m_{AE} = \frac{\dot{n}_{vac} \times 28.98 \times 2.20462}{1000}$$

The vacuum pressure (P_{vac}) in mmHg can then be determined, with P_{des} being the desorption pressure in bar_a.

$$P_{vac} = P_{des} \times 750.062$$

The vacuum factor can then be determined.

$$VF = \frac{m_{AE}}{P_{vac} \cdot N_{vac}}$$

ICF	PCF	CCF	ECF	FCF	BCF	LCF
3	6	4	0	1	2	0

Vacuum pump motors

The cost correlation in Garrett for vacuum pumps does not include the motor. The cost of the motor is obtained from P&T.

Where W_S is the shaft work of the motor in kW, costs are for a totally enclosed fan cooled (TEFC) motor.

$$C_{eqpt} = -0.05344 \cdot W_S^2 + 104.737 \cdot W_S + 448.863$$

ICF	PCF	CCF	ECF	FCF	BCF	LCF
1	0	0	4	0	0	0

Control valves

The cost correlation for carbon steel gate valves is from P&T, where D is the diameter of the valve in metres.

$$C_{eqpt} = \exp(11.45291) \times D^{2.720508}$$

A gas velocity of 12 $m \cdot s^{-1}$ was assumed to determine the pipe size. It is also assumed that all CVs have the same size.

$$A_{CV} = \frac{\dot{m}_{feed}^{total}}{\rho_{T_{ads},P_{ads}}^{gas} \times 12}$$

$$D_{CV} = \sqrt{\frac{4 \cdot A_{CV}}{\pi}}$$

The diameter is limited to 0.85 m if the result is larger.

ICF	PCF	CCF	ECF	FCF	BCF	LCF
2	4	2	0	0	0	0

There are 3 CVs per bed, so the total cost is given by:

$$C_{total} = C_{ins} \times 3 \times N_{beds}^{CapEx} \times \frac{CE_{PV}}{CE_{PT}} \times ER_{PV}$$

Operating costs

Electricity

The contributions to electricity consumption are the cooling water pumps, compressors, and vacuum pumps.

The electrical power consumption of the cooling water pump was estimated by assuming a 75 % hydraulic efficiency, and an 85 % motor & drive efficiency.

$$\dot{E}_{CW} = \frac{Q_{CW} \times \Delta P_{CW}}{\eta_{pump} \cdot \eta_{elec}}$$

The electrical power consumption of the compressors was estimated by their shaft work requirements, which already includes an 83 % efficiency for the compressor, and 90 % efficiency is assumed for the motor & drive. These values are appropriate for large units, however, should be adjusted for each application.

$$\dot{E}_{comp} = \frac{W_S}{\eta_{elec}} \times N_{comp}$$

The electrical power consumption of the vacuum pumps was taken from the manufacturer's specification. In the case of the Pfeiffer Okta 18000, 45 kW per pump, and 15 kW per pump for the Okta 4000.

$$\dot{E}_{vac} = \dot{E}_{vac}^{each} \times N_{vac}$$

The power requirements were then converted to energy requirements per year, as the natural gas is costed per GJ. A round-trip efficiency of 55 % was assumed for the generation of this electricity from an NGCC process/CHP plant.

$$E_{tot} = \left(\dot{E}_{CW} + \dot{E}_{comp} + \dot{E}_{vac}\right) \times \frac{3600 \times 24 \times 365}{10^6}$$

$$E_{NG} = \frac{E_{tot}}{0.55}$$

$$C_{Op}^{NG} = E_{NG} \times C_{NG}$$

The cost of natural gas was taken as 4 USD·GJ^{-1} from Brennan[36]. This was adjusted from a 1996 basis using the 1996 CEPCI of 381.7, and then converted to GBP using the exchange rate previously mentioned.

Cooling water

The cooling water flow rate was also converted to a per annum basis.

The cost of recirculated cooling water was taken as 0.05 USD·m^{-3} from Brennan and also adjusted to current day values in the same way as described above.

Steam

The steam consumption (mass flow rate) was also converted to a per annum basis.

The cost of high-pressure steam was taken as 15 USD·t^{-1}, and also converted to current day costs using the method described for the cost of natural gas.

Adsorbent replacement

It was assumed that the adsorbent had a lifetime of 5 years.

The total installed cost of adsorbent was divided by 5 and assigned as an annual operating cost.

CO_2 capture cost

The total capital cost (C_{Cap}) is given by the sum of the installed capital costs for the listed equipment items. The annual operating costs (C_{Op}) are given by the sum of the operating costs presented.

The capital recovery factor (CRF) is calculated for an interest rate (i) of 10 %, and a payback period (n) of 25 years.

$$CRF = \frac{i \cdot (1+i)^n}{(1+i)^n - 1}$$

The CRF is then used to annualise the total capital cost, such that a total annual cost (TAC) can be obtained.

$$TAC = CRF \cdot C_{Cap} + C_{Op}$$

The TAC is then used to determine the capture cost per tonne of CO_2 (CCPT), where $TPDc_{CO2}$ is the tonnes of CO_2 captured per day.

$$CCPT = \frac{TAC}{TPDc_{CO_2} \times 365}$$

Absorption model

The absorption model is based on the conventional amine absorption process layout. There are limits imposed on the maximum size of unit operations, and as such depending on the application there may be multiple unit operations. There are almost always multiple heat exchangers due to limitations in maximum area. To facilitate this, storage tanks have been included at points to allow the distribution of fluid to the multiple unit operations. The tanks are sized based on residence time for each application.

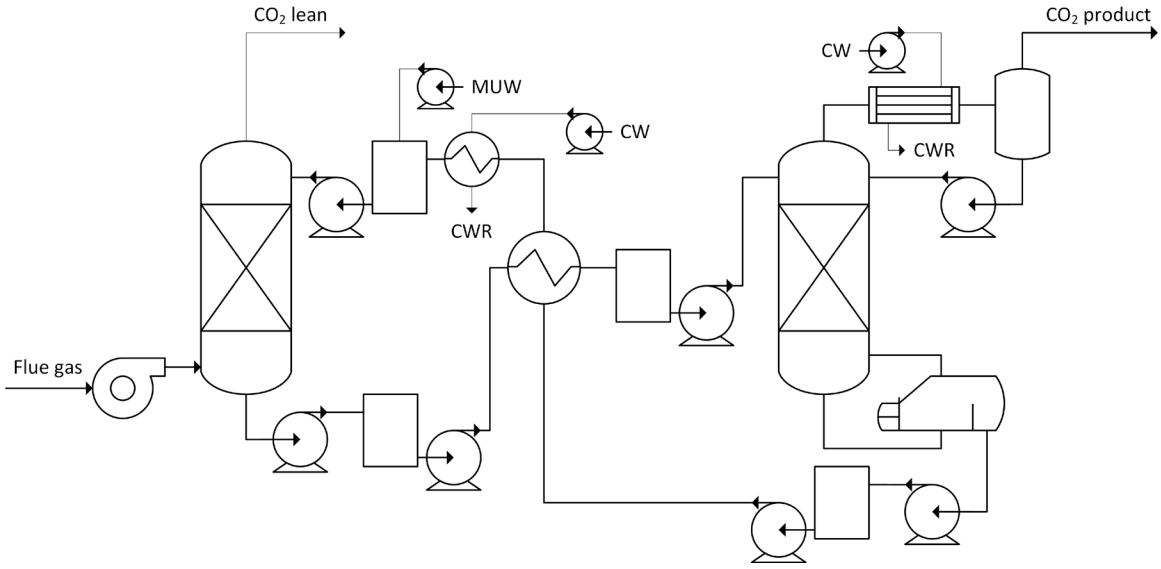

Figure 35 – Process equipment considered for design and costing in the absorption model

The absorption model is not a rigorous/discretised rate-based model, but rather rates are calculated based on inlet/outlet conditions. This returns more accurate results than a fully equilibrium model as the process is kinetically limited, however, temperature profiles are not able to be generated and accounted for. Although this model would not be suitable for rigorous process design, it has sufficient accuracy to enable a costing comparison.

In this work, MEA was compared to Cansolv, also an amine-based absorbent with lower regeneration energy requirements. This comparison is not straightforward as there are many conflicting reports in the literature. It was assumed that the physical properties and reaction characteristics of Cansolv were the same as MEA, with the only difference being the reboiler energy requirements. The work by Just[41] was the only one in why MEA was directly compared to Cansolv in the same apparatus under the same conditions. Their results were used as the scaling factor between the two in this work.

There are some parameters which remain constant through the process:

CO_2 recovery/capture rate (CR)	90 $\%_{mol}$
Amine concentration (C_{am})	30 $\%_{wt}$
Lean amine loading	0.08 mol(CO_2)·mol(amine)$^{-1}$
Flue gas pressure	1.05 bar_a
Absorption temperature (T_F)	40 °C
Absorber flooding (F_{OP}^{abs})	70 %
Regenerator flooding (F_{OP}^{reg})	70 %
Approach to equilibrium	90 %
Condenser molar reflux ratio	2
Regenerator overhead pressure drop (P_{loss})	2 psi
Reboiler steam temperature	406.7 K (3 bar_a saturated)

A range of lean loadings were investigated, and it was determined that 0.08 mol·mol^{-1} was close to the minimum cost in each case.

The feed pressure to the absorber was adjusted on a case by case basis, such that the blower work could be minimised. The results of this are presented in the table below. It was assumed that the temperature rise in the blower was negligible, so the absorption temperature is the same as the flue gas temperature.

Absorber feed pressure for each scenario [bar_a]	
Natural gas	1.08
Coal	1.06
Cement	1.06
Steel	1.06

The gas inlet pressure is selected such that the outlet pressure from the absorber was at least 1.05 bar_a. The method used to calculate the pressure drop is described later.

It was assumed that the column could achieve 90 % of the equilibrium loading value once kinetics were accounted for. This was used when determining the lean amine circulation rate.

It was required to assume a condenser reflux ratio in order to solve the energy balance. This is an area that does not receive much attention in other work, as the condenser requirements are generally excluded. As such there is no guideline for these values. It was assumed that the reflux ratio between condensed water reflux, and CO_2 product gas on a molar basis was 2.

The regenerator overhead pressure drop is what the fluid experiences between the regenerator overhead outlet, and the reflux drum.

A range of resources were used during the development of the model and will be highlighted accordingly, however, whenever Kohl[42] and the GPSA Databook[34] are used, the correlations are design data are in imperial units. Care should be taken around the unit conversion when indicated. A range of conversion factors is provided below.

1	kPa	=	0.145038	psi
1	bar	=	14.5038	psi
1	kg	=	2.20462	lb
1	m	=	3.28084	ft
1	m^3	=	35.3147	ft^3
1	BTU	=	1.05506	kJ

Throughout the process, various design correlations, and physical and chemical properties are required. To expediate the process a number of sub-function were developed and used throughout the model when required. These will be indicated when used (highlighted in red) and are provided at the end of this section under "Sub-functions".

For physical properties such as density, heat capacity, and viscosity of the gas mixtures, data was generated in HYSYS using the PR-EOS and numerically fit to functions in order to enable data generation in the model on-the-fly. For the same properties of water, and also the heat of vapourisation, data was obtained from the NIST Thermophysical Properties of Fluid Systems database[43], and also numerically fit.

Absorber design

The first step is to undertake a mass and energy balance to determine the flow rate of lean amine required. This is based on the method provided in Kohl[42].

The absorber design is an iterative process, both from an energy balance (EB) and pressure drop (DP) perspective, i.e. the outlet pressure is first assumed to obtain the driving force over the column, then the actual pressure drop is calculated, and the process iterated until convergence. We used 1 % as a convergence criteria.

The heat of reaction of CO_2 with MEA is taken as 825 $BTU \cdot lb_{CO2}^{-1}$, from Table 2-11 of Kohl.

The first step is to calculate the total heat of reaction, W_{CO2}^{feed} is the CO_2 mass flow rate in the feed gas in $lb \cdot hr^{-1}$.

$$Q_{RX} = W_{CO_2}^{feed} \cdot \Delta H_{RXN}$$

The lean amine inlet temperature (T_L) is set 10 °F above the gas inlet temperature:

$$T_L = T_g + 10$$

To begin the convergence loop, assume the rich amine temperature (T_R) is 36 °F above the lean temperature: $T_R = T_L + 36$

The calculated value for rich amine outlet temperature from the energy balance is then used as the starting value. For the pressure drop loop, the outlet pressure is first assumed to be 0.02 bar less than the gas inlet pressure.

BEGIN DP LOOP

BEGIN EB LOOP

- First, solve rich loading of amine such that the CO_2 vapour pressure is equal to the CO_2 partial pressure in the feed, at T_R. The VLE relationship of Gabrielsen[44] was used.
- Calculate amine acid gas pick up(AGPU) (or working capacity): rich loading – lean loading.
- Calculate the lean amine mass flow rate (W_L), where n_{CO2}^{feed} is the molar flow rate of CO_2 in the feed in mol·hr^{-1}, where MW_{amine} is the molar mass of MEA in lb·mol^{-1}, to give W_L in lb·hr^{-1}:

$$W_L = \frac{\dot{n}_{CO_2}^{feed} \times CR \times MW_{\text{amine}}}{AGPU \times C_{am}/100}$$

- Calculate the wet composition of the outlet gas at the lean amine temperature, and outlet pressure.
- Calculate the heat capacity of the outlet gas (C_P^{outlet}) assuming an ideal mixture.
- Calculate the ratio: $r = \frac{A}{B} = \frac{W^{outlet} \times C_P^{outlet}\left(T_L, P^{outlet}\right)}{W_L \times C_P^{\text{amine}}\left(T_L\right)}$ where W^{outlet} is the mass flow rate of the outlet gas stream, and W_L is the mass flow rate of lean amine. If r > 1, the assumption that the outlet gas is at the lean amine temperature is invalid. There is a detailed approach to deal with this in Kohl[42], however, the immediate solution is to

increase the amine circulation rate (W_L) by an appropriate factor. This was not required for the scenarios investigated here, but this issue may arise at very small scales.

- Calculate water evaporation or condensation: $W_{H_2O} = W_{H_2O}^{feed} - W_{H_2O}^{outlet}$
- Calculate associate heat of water phase change: $Q_{H_2O} = W_{H_2O} \times \Delta H_{lv}$
- Calculate rich amine mass flow rate: $W_R = W_L + W_{CO_2}^{feed} \cdot CR + W_{H_2O}$
- Calculate CO_2 loading of rich amine in lb(CO_2) per 100 lb(amine), C_{AG}^{rich}
- Calculate heat capacity of rich amine: $C_P^{rich} = C_P^{amine}(T_L) - 0.0068182 \times C_{AG}^{rich}$. The constant in this equation is the slope of the lines in figure 2-77 of Kohl.
- Calculate the rich amine temperature based on the energy balance:

$$T_R^{calc} = \frac{B \cdot (T_L - T_F) - A \cdot (T_P - T_F) + Q_{RX} + Q_{H_2O}}{C_P^{rich} \cdot W_R} + T_F$$

- Calculate error: $err = \left| \frac{T_R - T_R^{calc}}{T_R} \right|$

END EB LOOP

- Assume 90 % of the equilibrium rich loading is going to be achieved.
- Calculate new energy balance from lean amine flow rate onwards, and obtain 'actual' T_R.
- Size absorber diameter based on the GPDC method, impose limit of 16 m on absorber diameter.
    - Using Mellapak 2X structured packing
    - Packing properties from Green & Southard[45]. Packing factor = 23, surface area = 223 $m^2 \cdot m^{-3}$, void fraction = 0.99.
    - Packing dimensions (for interfacial area calculations) from Wang et al.[46]. Channel base width (B) = 0.0302 m, crimp height (h) = 0.0143 m, corrugation angle = 60 °. We assumed the surface enhancement factor (F_{SE}) to be the same as that for other similar packings from Rocha et al.[47], F_{SE} = 0.350.
- Calculate flooding point for packing: $\Delta P^{flood} = 0.12 \times F_p^{0.7}$
- Calculate F_{LG}: $F_{LG} = \frac{\dot{m}_L}{\dot{m}_g} \sqrt{\frac{\rho_g(T_L, P_g, y_{feed})}{\rho_L(T_L)}}$ where m_L is the mass flow rate of lean amine in $kg \cdot s^{-1}$, m_g is the mass flow rate of feed gas, ϱ_g is the gas density in $kg \cdot m^{-3}$ at the inlet conditions, and ϱ_L is the density of the lean amine.

- Calculate the capacity factor from the Kister & Gill GPDC correlation at the flooding point (F_{LG}, ΔP^{flood}) for structured packing. The GPDC chart[45,48] was digitised and the data fit with a model in order to automate the process. The function is provided at the end.

  Calculate superficial velocity (u_s) at operating flooding point:

$$u_s = \frac{CP}{\sqrt{\rho_g / \left(\rho_L - \rho_g\right)} \times \sqrt{F_P} \times \nu_L^{0.05}} \times F_{OP}^{abs}$$

  Superficial velocity is in $ft \cdot s^{-1}$. Densities are in $kg \cdot m^{-3}$, and ν_L is the viscosity of the MEA solution in cSt. A function was generated by digitising the data in Figure 2-68 in Kohl for the viscosity of 30 $\%_{wt}$ MEA solution.

BEGIN AD LOOP

- Convert superficial velocity (u_s) to $m \cdot s^{-1}$ and calculate column diameter:

$$A_C = \frac{\dot{m}_g}{\rho_g \cdot u_s \cdot N_{abs}}$$

$$D_C = \sqrt{\frac{4 \cdot A_C}{\pi}}$$

  Where m_g is the mass flow rate of the feed gas, and N_{abs} is the number of absorbers (initially 1).

- If $D_C > 16$ m, add another column.

END AD LOOP

- Calculate operating pressure drop of packing: solve the GPDC function for ΔP given F_{LG} and CP.
- Calculate amount of CO_2 to be absorbed per absorber: $n_{CO_2} = \dot{n}_{CO_2}^{feed} \times CR / N_{abs}$
- Calculate log mean values for temperature and CO_2 mole fraction across the column

BEGIN AH LOOP

- Calculate log mean value for pressure
- Calculate height of packing required to absorb n_{CO2}. Using mass transfer relationship (equation 11) from Mota-Martinez et al.[49]
  - The diffusivity of CO_2 in the liquid was calculated using the Wilke-Chang correlation[50]. The viscosity of pure MEA was calculated using the correlation of

DiGuilio et al.[51]. The molar volume of CO_2 at the normal boiling point (15549.2 $cm^3 \cdot mol^{-1}$) was interpolated from Din[52]. The values of φ for water and MEA were taken as 2.6 and 2.26 respectively.

- The pseudo first order reaction rate between CO_2 and MEA was taken from Penny & Ritter[53].
- The interfacial concentration of CO_2 was calculated using the Henry constant method of Penttilä et al.[54].
- The packing interfacial area was determined using the method of Shi & Mersmann[55], as interpreted by Rocha et al[47].
- The surface tension of the lean amine was obtained from the data provided by Vázquez et al.[56]. The data was fit with an equation in order to enable automation and interpolation, provided below.

- Calculate number of packing sections required using a maximum of 6 m/20 ft per section – based on the recommendation of the GPSA Databook[34].
- Calculate pressure drop of packing using operating pressure drop determined earlier. Calculate pressure drop due to liquid distributors (one per section) using method from Rix & Olujic[57]. Assume pressure drop of packing supports is negligible.
- Determine gas outlet pressure at the end of the "active packing" section.
- Calculate error between calculated outlet pressure and assumed outlet pressure.

END AH LOOP

- Calculate error between calculated outlet pressure and the initially assumed outlet pressure.

END DP LOOP

- Check lean loading.
  - Calculate vapour pressure of CO_2 over amine solution at 'final value' of outlet pressure.
  - If MEA lean loading is too high (partial pressure of CO_2 due to VLE is greater than desired CO_2 partial pressure in the outlet) – restart process with lower lean loading.
- Calculate pressure drop above active packing section.
  - Calculate pressure drop due to water wash section.

        - Use GPDC method with the specified water wash flow rate, and the gas outlet flow rate.
        - Assume 1.5 m of water wash packing height.
    - Calculate pressure drop due to demister, using method of Setekleiv and Svendsen[58]. Assuming a demister thickness of 0.30 m.
        - Using Sulzer 9030-L2[59], surface area = 482 $m^2 \cdot m^{-3}$, density = 144 $kg \cdot m^{-3}$, and void fraction = 0.98.
    - Calculate pressure drop due to water wash collection tray, using method from Rix & Olujic[57].
- Calculate final gas outlet/vent pressure. Pressure at outlet of active packing minus pressure drop due to components above active packing.
- Calculate tan-tan height of absorber:

$$Z_{TT}^{abs} = Z_{pack} + Z_{ww} + Z_{dem} + \left(N_{\text{sec}} + 4\right) \times 0.9 + Z_{duct} + Z_{LHU}$$

Z_{pack} is the total active height of packing, Z_{ww} is the height of water wash packing, Z_{dem} is the thickness of the demister pad, 3 ft allowances between sections for column ancillaries, inlet, outlet, above packing section, Z_{duct} is the height due to the flue-gas inlet duct, and Z_{LHU} is the height of liquid hold up.

- Assume 20 $m \cdot s^{-1}$ gas velocity in the flue gas duct.
- Assume 5 minutes of liquid hold up.

Regenerator design

The regenerator design is based on an energy balance which is used to obtain the required stripping steam flow rate. Then this is used for the process design.

- Regenerator bottom T and P set by lean amine specifications.
    - Bottom temperature (T_{rg}^{btm}) (assume same as reboiler temperature) from Figure 2-88 in Kohl – digitised and provided as a function.
    - Bottom pressure (P_{rg}^{btm}) is set by amine solution vapour pressure at that temperature. From figure 2-56 in Kohl – digitised and provided as a function.
- Calculate rich amine outlet temperature from lean-rich exchanger – rich amine inlet temperature to regenerator (T_{in}^{rich}).
    - Lean amine inlet temperature is regenerator bottom temperature
    - Rich amine inlet temperature is absorber bottom temperature
    - Lean amine outlet temperature is 40 °F/22°C above rich amine inlet temperature
- Assume initial regenerator overhead pressure, and then loop design to convergence: $P_{RO} = P_{BTM} - 1$ psi.

BEGIN RD LOOP

- Set condenser pressure to: $P_{cond} = P_{RO} - P_{loss}$

BEGIN CEB LOOP

To solve the regenerator energy balance simultaneous equations:

$$Q_{cond} = Q_{cond}^{lat} + Q_{cond}^{sens}$$

$$Q_{reb} = Q_{cond} + Q_{RX} + \dot{m}^{rich} \times C_P^{rich} \times \left(T_{rg}^{btm} - T_{in}^{rich}\right)$$

The latent heat contribution (Q_{cond}^{lat})to the condenser energy balance is unknown, and is the variable to be solved. Q_{cond}^{lat} is unknown as the water content and temperature of the regenerator overhead stream is unknown. The objective function is the reflux ratio of regenerator, i.e. Q_{cond}^{lat} is solved to give the desired reflux ratio.

The reboiler energy balance equation is the typical format[42,60].

- Perform condenser energy balance:
    - Calculate water content of product gas (m_{out}^{H2O}) at the condenser temperature, using its saturation pressure and Raoult's law.
    - Calculate composition of outlet gas assuming only H_2O and CO_2 are present. The flow rate of CO_2 in the outlet gas on a dry basis is known, as it is the amount of CO_2 absorbed/desorbed.

- Calculate regenerator overhead water content: $\dot{m}_{RO}^{H_2O} = \frac{Q_{cond}^{lat}}{\Delta H_{lv}} + \dot{m}_{out}^{H_2O}$
- Calculate composition and flow rate of regenerator overhead stream
- Calculate temperature of regenerator overhead (T_{RO}) stream using the partial pressure of H_2O in the overhead stream (its corresponding saturation temperature).
- Calculate sensible heat requirements of condenser:

  $Q_{cond}^{sens} = \dot{m}_{RO} \times C_P^{RO} \times \left(T_{RO} - T_{cond}\right)$

  A function is provided for the heat capacity of a CO_2/H_2O mixture.
- Calculate condenser and reboiler duties
- Calculate reflux ratio – on a molar basis between the flow rate of the CO_2 product stream (wet basis) and the water reflux returning to the column. Water present in the regenerator overhead that does not exit with the CO_2 product returns as reflux.
- Calculate error: $err = RR - RR_{calc}$

END CEB LOOP

- Use calculated reboiler duty to obtain stripping steam flow rate assuming reboiler duty only vapourises H_2O, using the enthalpy of vapoursation at the reboiler pressure:

$$\dot{m}_{H_2O}^{boilup} = \frac{Q_{reb}}{\Delta H_{lv}\left(P_{rg}^{btm}\right)}$$

- Calculate diameter of regenerator and pressure drop using the same method described for the absorber.
  - The gas flow rate of the active packing section is the steam flow rate, the liquid flow rate is the rich amine flow rate.
  - For the regenerator, the reflux liquid is used as the water wash.
- Calculate error between calculated overhead pressure and initially assumed overhead pressure.

END RD LOOP

- Check that the actual condenser pressure is above the required limit, 1.05 bar_a used in this work: $P_{cond}^{calc} = P_{RO}^{calc} - P_{loss}$

- If it is below the limit, the flooding percentage could be adjusted, or the lean amine loading could be reduced in order to increase the bottom pressure.

- Calculate tan-tan height if regenerator using same method described for the absorber.
  - For the regenerator, $Z_{duct} = 0$

Sub-functions

GPDC chart/correlation

Data from Kister et al.[45,48]

Range: 0.005 ≤ FLG ≤ 2 and 0.25 ≤ ΔP ≤ 1.5 $in_{H2O} \cdot ft^{-1}$

$$u = \ln\left(F_{LG}\right) \qquad v = \Delta P$$

$$CP = x_1 \cdot u + x_2 \cdot v + x_3 \cdot \ln\left(v\right) + x_4 \cdot \exp\left(u\right) + x_5 \cdot \exp\left(v\right) + x_6 \cdot u^2 + x_7 \cdot u^3 \ldots$$
$$+ x_8 \cdot u \cdot v + x_9 \cdot \left(u \cdot v\right)^2 + x_{10} \cdot \left(u \cdot v\right)^3 + x_{11} \cdot \left(u \cdot v\right)^4 + x_{12} \cdot u \cdot v^{-1} + x_{13}$$

Where:

x_1 = -0.757736978 x_2 = 0.607599649 x_3 = -0.0808 x_4 = 0.307567553

x_5 = -0.141355268 x_6 = -0.110693574 x_7= -0.0084 x_8 = 0.0739

x_9 = 0.00255 x_{10} = -0.00425 x_{11} = -0.000428

x_{12} = 0.0433 x_{13} = -0.0114.

Amine solution viscosity (ν_L)

Data from Figure 2-68 in Kohl[42].

Range: 280 ≤ T ≤ 378 K

$$\nu_L = \exp\left(2.49942 \cdot 10^{-7} \times T^3 - 2.0028 \cdot 10^{-4} \times T^2 + 3.994739 \cdot 10^{-2} \times T - 0.357760296\right)$$

Where ν_L is in cSt.

MEA surface tension (σ_L)

$$K_1 = \frac{76.08923 + 1151.03744 \cdot x}{1 + 19.12543 \cdot x + 2.96876 \cdot x^2}$$

$$K_2 = -0.1609 - 0.00391 \cdot x^{0.86347}$$

$$\sigma_L = \frac{K_1 - K_2 \cdot T}{1000}$$

Where x is the molar fraction of MEA in the amine solution, and T is the temperature of the solution in °C.

Amine regeneration temperature

Data from Figure 2-88 in Kohl[42].

Range: $0.015 \leq \alpha \leq 0.32$ mol·mol^{-1}

$$T = -41.1285 \times \ln(\alpha) + 156.4586$$

T is in °F

Amine saturation pressure

Range: $220 \leq T \leq 365$ °F

$$P^{\circ}_{\text{amine}} = \exp\left(\frac{-8827.73192}{T + 459.67} + 15.68753\right)$$

$P_{amine}°$ is in psia.

Rich amine density

Data from Amundsen et al.[61]. Function applies for 30 $\%_{wt}$ MEA only.

Range: $25 \leq T \leq 80$ °C, $0.1 \leq \alpha \leq 0.5$ mol·mol^{-1}

$$\rho_{MEA}^{rich} = 1000 \times \left[x_1 \cdot T + x_2 \cdot \alpha + x_3 \cdot \exp(\alpha) + x_4 \cdot T^2 + x_5 \cdot \alpha^4 + x_6 \cdot T \cdot \alpha + x_7 \right]$$

Where ϱ_{MEA}^{rich} is in kg·m^{-3}.

Where:

$x_1 = -0.00041288315$ $x_2 = -0.19127554$ $x_3 = 0.335208741$

$x_4 = -1.4389298 \cdot 10^{-6}$ $x_5 = -0.223756005$ $x_6 = 7.493324 \cdot 10^{-5}$

$x_7 = 0.688011038$

Rich amine viscosity

Data from Amundsen et al.[61]. Function applies for 30 $\%_{wt}$ MEA only.

Range: 25 ≤ T ≤ 80 °C, 0.1 ≤ α ≤ 0.5 mol·mol^{-1}

$$\mu_{MEA}^{rich} = x_1 \cdot T + x_2 \cdot \alpha + x_3 \cdot \exp(\alpha) + x_4 \cdot T^2 + x_5 \cdot T^3 + x_6 \cdot T \cdot \alpha$$

Where:

x_1 = -0.146305695 x_2 = -3.222437162 x_3 = 5.225757408 x_4 = 0.001708255

x_5 = -6.891501·10^{-6} x_6 = -0.03563098

Cost estimation

The method is the same as that described for the adsorption model. Information pertaining specifically to the absorption model is presented.

Feed blower

The feed blower work is calculated using the isentropic work formula:

$$P_2 = P_{FG} + \Delta P_{duct}$$

$$E_{blower} = \frac{1}{\eta_{isen}} \cdot \frac{k}{k-1} \cdot R \cdot T \cdot \left[\left(\frac{P_2}{P_{FG}} \right)^{\frac{k-1}{k}} - 1 \right]$$

$$W_s = \frac{E_{blower}}{MW_{feed}} \times \dot{m}_{feed}$$

Where P_{FG} is the feed/delivery pressure of the flue gas, and ΔP_{duct} is the pressure loss of the duct – assumed to be 0.03 bar.

If the volumetric flow rate of the feed is > 15 $m^3 \cdot s^{-1}$, opt for a typical induced draught fan as used in power plant/boiler application. Given cost correlations do not exist for these units, cost the unit as an motor driven centrifugal compression – as the shaft work requirements are in the same order of magnitude and the manufacturing process is similar.

If the volumetric flow rate of the feed is < 1000 $m^3 \cdot s^{-1}$ (based on manufacturer characteristic curves[62]), use one blower to feed all absorbers. Otherwise $N_{blower} = N_{absorbers}$.

Use cost correlation for compressor in adsorption model section for purchase cost estimation.

If volumetric flow rate of feed is ≤ 15 $m^3 \cdot s^{-1}$, cost unit as a blower ($N_{blower} = 1$). Cost correlation for a blower with a maximum outlet pressure of 0.69 bar from P&T – where Q is the volumetric flow rate in $m^3 \cdot s^{-1}$.

$$C_{eqpt} = \exp(10.94457426) \times Q^{0.606200979}$$

ICF	PCF	CCF	ECF	FCF	BCF	LCF
3	6	4	4	2	3	0

Absorber

- The cost of 1 absorber (absorber + internals) is first calculated and then multiplied by N_{abs}.
- Calculate mass of packing required:

$$m_{pack} = A_C \cdot \left(Z_{pack} + Z_{ww}\right) \cdot \left(1 - \varepsilon_{pack}\right) \cdot 8000$$

  Where 8000 represents the density of 304 SS.
- Calculate the thickness of the vessel using method described in adsorption column section
  - Mass of adsorbent is replaced with mass of packing
  - f = 133 MPa for PT460 steel at 100 °C
- Calculate mass of steel required using method described in the adsorption column section.
- Use same cost correlation for carbon steel column in the adsorption column section.

ICF	PCF	CCF	ECF	FCF	BCF	LCF
4	4	4	1	1	2	2

Absorber internals

Packing

Costs were taken from Wang et al.[63]. Costs are on a 2014 basis, therefore a CEPCI of 576.1 should be used when adjusting the cost to the present-day value.

$$C_{eqpt} = \left(7.31 \times A_{pack} + 203.05\right) \cdot V_{pack}$$

Where A_{pack} is the surface area of the packing in $m^2 \cdot m^{-3}$, and V_{pack} is the volume of packing required in m^3.

ICF	PCF	CCF	ECF	FCF	BCF	LCF
3	0	0	0	0	0	0

Packing supports

Costs were taken from Wang et al.[63]. Costs are on a 2014 basis, therefore a CEPCI of 576.1 should be used when adjusting the cost to the present-day value.

$$C_{eqpt} = \left(12019 \times D_C^{0.1792}\right) \times \left(N_{\text{sec}} + 1\right)$$

Where D_C is the diameter of the column in m.

ICF	PCF	CCF	ECF	FCF	BCF	LCF
3	0	0	0	0	0	0

Liquid distributors

Costs were taken from Wang et al.[63]. Costs are on a 2014 basis, therefore a CEPCI of 576.1 should be used when adjusting the cost to the present-day value.

$$C_{eqpt} = \left(1 + 5/6\right) \cdot 15335 \times D_C^{0.1764} \times \left(N_{\text{sec}} + 1\right)$$

Where D_C is the diameter of the column in m.

ICF	PCF	CCF	ECF	FCF	BCF	LCF
3	0	0	0	0	0	0

Demister pad

Costs were taken from Vatavuk[64]v. Costs are on a 1988 basis, therefore a CEPCI of 342.4 should be used when adjusting the cost to the present-day value.

$$C_{eqpt} = 78.4 \times D_C^{1.66} \times \left(Z_{dem} / 0.15 \right)$$

Where D_c is the diameter of the absorber in feet, and Z_{dem} is the thickness of the demister in m.

ICF	PCF	CCF	ECF	FCF	BCF	LCF
3	0	0	0	0	0	0

Regenerator

- The cost of 1 regenerator (absorber + internals) is first calculated and then multiplied by N_{reg}.
- Calculate mass of packing required
- Calculate the thickness of the vessel using method described in adsorption column section
    - Mass of adsorbent is replaced with mass of packing
    - f = 183 MPa for 304 SS at 200 °C.
- Calculate mass of steel required using method described in the adsorption column section. The variation in density between CS and SS 304 is not signi

Cost correlation for 304 SS columns from P&T based on shell mass (m) in kg.

$$C_{eqpt} = \exp\left(6.019165699\right) \times m^{0.642626314}$$

ICF	PCF	CCF	ECF	FCF	BCF	LCF
4	5	4	1	1	2	3

Regenerator internals

Same procedure as per absorber internals.

Lean-Rich Exchanger(s)

- Calculate the total area required based on the total duty from the regenerator energy balance calculations.
    - Assumed overall heat transfer coefficient, U = 900 $W \cdot m^2 \cdot K^{-1}$
- Determine number of exchangers based on a maximum area of 1500 m^2 per exchanger.

Cost correlation for shell & tube heat exchanger with SS shell and tubes up to 100 psi_a, from P&T.

$$C_{eqpt} = \exp(7.169723) \cdot A^{0.726108}$$

ICF	PCF	CCF	ECF	FCF	BCF	LCF
2	3	4	1	1	1	2

Reboiler(s)

- Calculate total area required based on reboiler heat duty from regenerator energy balance.
    - Assumed overall heat transfer coefficient, U = 1500 $W \cdot m^2 \cdot K^{-1}$
    - This will also give the required steam utility flow rate.
- Determine number of exchangers based on a maximum area of 1500 m^2 per exchanger.
- If $N_{reb} < N_{reg}$, force $N_{reb} = N_{reg}$ (unlikely to be required)
    - Adding another condition so that each regenerator has the same number of reboilers is a possibility for added peace of mind. However, in this work an evenly divisible number of reboilers always resulted.

The cost correlations for the reboilers, are from Corripio et al.[65]. Using a kettle type made from 304 SS, up to 100 psig shell/kettle side. The costs are on a 1979 basis with an Equipment CEPCI of 252.5. The corresponding Equipment CEPCI value for 2000 is 438 – required when determining installation cost factors. The CEPCI for 1979 is 238.7 – required when converting installed cost to current day value.

$$C_{eqpt} = F_d \cdot F_m \cdot \exp\left[8.202 - 0.01506 \cdot \ln(A) + 0.06811 \cdot \ln^2(A)\right]$$
$$F_d = 1.35$$
$$F_m = 1.1991 + 0.15984 \cdot \ln(A)$$

Where A is the area of the heat exchanger in m^2.

N.B. – The installation cost factors are on a carbon steel basis, therefore, when looking up the table, $F_m = 1$.

ICF	PCF	CCF	ECF	FCF	BCF	LCF
2	5	4	1	1	2	3

For the Cansolv case, the process was repeated except the reboiler duty was scaled based on the scaling factor of 2.7/4.0 from Just[41], and later calculations which rely on this value such as steam requirements and exchanger area/cost are repeated with this duty.

Condenser(s)

- The condensers are costed in the same way as the lean-rich exchangers.
- The area can be obtained from the condenser duty from regenerator energy balance.
    - Assumed overall heat transfer coefficient, U = 200 $W \cdot m^2 \cdot K^{-1}$
    - Cooling water inlet temperature (T_{CW}^{in}): 298.15 K
    - Cooling water return temperature (T_{CW}^{out}): 303.15 K
    - Condenser minimum approach temperature (T_{app}): 10 K
    - Condenser temperature = $T_{CW}^{out} + T_{app}$
- This will also give the required cooling water flow rate.

ICF	PCF	CCF	ECF	FCF	BCF	LCF
2	5	4	1	1	2	2

Lean amine cooler(s)

- Calculate duty and area requirements
    - From the regenerator energy balance, the temperatures of all four streams are known.
    - The flow rates of all the streams are also known.
    - Assumed overall heat transfer coefficient, U = 900 $W \cdot m^2 \cdot K^{-1}$
- Calculate number of exchangers based on a maximum area per exchanger of 1500 m^2.
- If $N_{LAC} < N_{LR}$, set $N_{LAC} = N_{LR}$, this will make fluid distribution and piping requirements more straightforward.
- Unit is costed in the same way as the lean-rich exchanger.

ICF	PCF	CCF	ECF	FCF	BCF	LCF
2	3	3	1	1	2	2

It is not uncommon for the lean amine cooler and the condensers to be air-cooled units, however, given the duty requirements in the scenarios here, it was not feasible to do so.

Amine holding/distribution tanks

- Calculate volume for each of the four tanks & the reflux drum
    - Assume 600 s holdup time per tank
    - The total flow rate of each inlet stream to the tanks is known.
- Size and cost tanks as small (up to 2650 m^3) field erected tanks from P&T – API-650 tanks, SS 304
    - Also determine the height of the tanks (method provided below) as it is required later to approximate the pumping head requirements.

$$C_{eqpt} = 130.46 \times V_{\text{tank}} + 53432$$

ICF	PCF	CCF	ECF	FCF	BCF	LCF
4	5	3	1	1	1	2

Table of API-650 tank heights[66] to lookup based on volume.

Tank volume (m^3)		Tank height (m)
min	max	
	≤ 200	4.88
200	550	7.32
550	1300	9.75
1300	2500	12.2
2500	24000	14.6

Pumps

- Assume 10 kPa pressure loss (ΔP_{losses}) due to fittings and friction in each pipe section
- Assume 20 kPa pressure loss (ΔP_{HX}) in heat exchangers
- Assume 50 kPa pressure loss (ΔP_{CW}) over cooling water circuit
- In cases where the ΔP for a given pump is < 0 due to static head contributions, the cost of that pump is set to 0.
- For pumps that are indicated as stainless steel, a material factor of 1.7 is applied to the cost correlation for 304 SS.
    - Same cost correlation from P&T as per cooling water pumps in adsorption model section.
    - The same installation cost factor rows were used for all pumps

ICF	PCF	CCF	ECF	FCF	BCF	LCF
1	3	3	4	1	2	2

Absorber outlet to absorber outlet tank

Carbon steel construction

$$Q = \frac{V_{\text{tank}}}{t_{HU} \cdot N_{abs}}$$

$$\Delta P = \Delta P_{losses} + \rho \cdot g \cdot \left(Z_{AOT} - Z_{LHU}\right)/1000$$

Where V_{tank} is the volume of the absorber outlet tank, t_{HU} is the hold up time of the tank, and N_{abs} is the number of absorbers. Z_{AOT} is the height of the absorber outlet tank, and Z_{LHU} is the height of the liquid holdup section in the absorber.

$N_{pumps} = 2 \times N_{abs}$

Absorber outlet tank to heated rich amine tank via LR exchanger

Carbon steel construction

$$Q = \frac{V_{\text{tank}}}{t_{HU} \cdot N_{LR}}$$

$$\Delta P = 3 \cdot \Delta P_{losses} + \Delta P_{HX}$$

Where N_{LR} is the number of lean-rich exchangers. It is assumed the level in both tanks are the same.

$N_{pumps} = N_{LR} + 2$

Heated rich amine tank to regenerator inlet

Stainless steel construction

$$Q = \frac{V_{\text{tank}}}{t_{HU} \cdot N_{reg}}$$

$$\Delta P = \Delta P_{losses} + \rho \cdot g \cdot \left(Z_{RG} - Z_{AOT}\right)/1000 + \left(P_{RO} - 101.325\right)$$

Where N_{reg} is the number of regenerators, Z_{RG} the height of the regenerator excluding the height of the water wash section, Z_{AOT} represents the height of the heated amine tank as it is assumed to be the same as the absorber outlet tank, and P_{RO} is the regenerator overhead pressure in kPa_a.

$N_{pumps} = 2 \times N_{reg}$

Regenerator to hot lean amine tank

Stainless steel construction

$$Q = \frac{V_{\text{tank}}}{t_{HU} \cdot N_{reb}}$$

$$\Delta P = \Delta P_{losses} + \rho \cdot g \cdot \left(Z_{HLA} - 1\right)/1000$$

Where N_{reb} represents the number of reboilers, Z_{HLA} represents the height of the hot lean amine tank, and it is assumed the liquid level in the reboiler is 1 m above ground level.

$N_{pumps} = N_{reb} + 2$

Reflux pump

Stainless steel construction

$$Q = \frac{Q_{reflux}}{N_{reg}}$$

$$\Delta P = \Delta P_{losses} + \rho \cdot g \cdot \left(Z_{RG} - Z_{RD}\right)/1000$$

Where Q_{reflux} is the total reflux flow rate for all regenerators, and Z_{RD} is the height of the reflux drum.

$N_{pumps} = 2 \times N_{reg}$

Hot lean amine tank to cooled lean amine tank via LR exchangers

Stainless steel construction

$$Q = \frac{V_{\text{tank}}}{t_{HU} \cdot N_{LR}}$$

$$\Delta P = 3 \cdot \Delta P_{losses} + 2 \cdot \Delta P_{HX}$$

Where N_{LR} is the number of lean-rich exchangers

$N_{pumps} = N_{LR} + 2$

Cooled lean amine tank to absorber

Carbon steel construction

$$Q = \frac{V_{\text{tank}}}{t_{HU} \cdot N_{abs}}$$

$$\Delta P = \Delta P_{losses} + \rho \cdot g \cdot \left(Z_{abs} - Z_{HLA}\right)/1000 + \left(P_{abs}^{out} - 101.325\right)$$

Where Z_{abs} is the height of the absorber excluding the water wash section, Z_{HLA} represents the height of the cooled lean amine tank as it is assumed to be the same as the hot lean amine tank, and P_{abs}^{out} is the gas outlet pressure of the absorber in kPa_a.

$N_{pumps} = 2 \times N_{abs}$

Absorber water wash pump

Carbon steel construction

$$Q = Q_{WW}$$
$$\Delta P = \Delta P_{losses} + \rho \cdot g \cdot Z_{TT} / 1000 + \left(P_{abs}^{out} - 101.325 \right)$$

Where Q_{WW} is the water wash flow rate per absorber in $m^3 \cdot s^{-1}$, and Z_{TT} is the tan-tan height of the absorber.

$N_{pumps} = N_{abs} + 1$

Cooling water pumps for condensers

Carbon steel construction

$$Q = \frac{Q_{CW}}{N_{cond}}$$
$$\Delta P = \Delta P_{CW}$$

Where Q_{CW} is the total cooling water flow rate requirements in $m^3 \cdot s^{-1}$, and N_{cond} is the number of condensers.

$N_{pumps} = N_{cond} + 2$

Cooling water pumps for lean amine cooler

Carbon steel construction

$$Q = \frac{Q_{CW}}{N_{LAC}}$$
$$\Delta P = \Delta P_{CW}$$

Where Q_{CW} is the total cooling water flow rate requirements in $m^3 \cdot s^{-1}$, and N_{LAC} is the number of condensers.

$N_{pumps} = N_{LAC} + 2$

Make-up water pump

Carbon steel construction

$$Q = Q_{MUW} = \frac{\dot{m}_{H_2O}^{out}}{\rho}$$

$$\Delta P = \Delta P_{loss} + \rho \cdot g \cdot Z_{HLA} / 1000$$

Where Q_{MUW} is the total make-up water flow rate requirements in $m^3 \cdot s^{-1}$, which is equal to the amount of water lost with the CO_2 product stream, and Z_{HLA} represents the height of the cooled lean amine tank.

$N_{pumps} = 2$

First fill amine costs

- Determine amount of amine solution required
    - The liquid holdup of the packing for both the absorber and regenerator was determined using the correlation developed by Suess and Spiegel[67].
    - The volume of the holdup sections of the absorber and regenerator are also added.
    - A residence time of 120 s was assumed for the reboilers to obtain the holdup volume.
    - The volume of all amine holdup tanks are also summed.
- The amount of pure MEA required was calculated from the total volume of solution
- The cost of amine used was 1100 US$\cdot t^{-1}$

ICF	PCF	CCF	ECF	FCF	BCF	LCF
2	0	0	0	0	0	0

Operating costs

Reboiler steam

- The total steam flow rate for regeneration is converted to an annual basis
- A cost of steam of 13 US$·t^{-1} was used from Brennan, and converted to the current day value as described in the adsorption model operating cost section.
- The process is repeated with the Cansolv duty requirements.

Electricity

- Electricity requirements are made up of the pumps and the feed blower(s).

$$\dot{E}_{pumps} = \frac{\sum_k Q_k \cdot \Delta P_k \cdot N_k}{\eta_{pump} \cdot \eta_{motor}}$$

Where k represents each pump in the system, and Q and ΔP are the corresponding values used in costing the pumps. N represents the number of pumps that are in operation, η_{pump} represents the hydraulic efficiency of the pump and η_{motor} represents the efficiency of the motor. The same values as per the adsorption model are used, 0.75 and 0.85 respectively.

$$\dot{E}_{blower} = \frac{W_S^{blower}}{\eta_{motor}}$$

Where W_S^{blower} is the shaft work requirements of the blower calculated for cost estimation, and η_{motor} is the efficiency of the motor, 0.90.

The annual energy requirement in GJ is then calculated.

$$E_{tot} = \left(\dot{E}_{pumps} + \dot{E}_{blower}\right) \times \frac{3600 \cdot 24 \cdot 365}{10^6}$$

The amount and cost of natural gas required to produce that electricity is determined in the same was as per the adsorption model.

Cooling water

- The cooling water requirements for the condensers and lean amine coolers are summed.
- The annual cost is determined in the same way as per the adsorption model.

MEA makeup

- A value of 1.6 $kg(MEA) \cdot t(CO2)^{-1}$ was used to represent the amine losses[68]

Makeup water

- Makeup water requirements include both the makeup water requirements resulting from loses, and water required to dilute the makeup MEA.
- A cost of 0.8 $USD \cdot m^{-3}$ for towns water from Brennan was used to cost this water requirement. The costs were converted to present GBP using the same method described for other utilities in the adsorption model operating cost section.

CO_2 capture cost

- The same method described in the adsorption model was used.
    - The process was undertaken twice, once with the associated costs for MEA, and again with the costs of the Cansolv process.

References

1 A. Majumder, R. Jain, P. Banerjee and J. Barnwal, Development of a new proximate analysis based correlation to predict calorific value of coal, *Fuel*, 2008, **87**, 3077–3081.

2 S. V. Vassilev, K. Kitano and C. G. Vassileva, Some relationships between coal rank and chemical and mineral composition, *Fuel*, 1996, **75**, 1537–1542.

3 J. A. Mason, K. Sumida, Z. R. Herm, R. Krishna and J. R. Long, Evaluating metal–organic frameworks for post-combustion carbon dioxide capture via temperature swing adsorption, *Energy Environ. Sci.*, 2011, **4**, 3030.

4 P. D. C. Dietzel, V. Besikiotis and R. Blom, Application of metal–organic frameworks with coordinatively unsaturated metal sites in storage and separation of methane and carbon dioxide, *J. Mater. Chem.*, 2009, **19**, 7362.

5 J. Moellmer, A. Moeller, F. Dreisbach, R. Glaeser and R. Staudt, High pressure adsorption of hydrogen, nitrogen, carbon dioxide and methane on the metal–organic framework HKUST-1, *Microporous Mesoporous Mater.*, 2011, **138**, 140–148.

6 Y. Chen, D. Lv, J. Wu, J. Xiao, H. Xi, Q. Xia and Z. Li, A new MOF-505@GO composite with high selectivity for CO2/CH4 and CO2/N2 separation, *Chem. Eng. J.*, 2017, **308**, 1065–1072.

7 P. D. C. Dietzel, R. Blom and H. Fjellvåg, Base-Induced Formation of Two Magnesium Metal-Organic Framework Compounds with a Bifunctional Tetratopic Ligand, *Eur. J. Inorg. Chem.*, 2008, **2008**, 3624–3632.

8 P. D. C. Dietzel, B. Panella, M. Hirscher, R. Blom and H. Fjellvåg, Hydrogen adsorption in a nickel based coordination polymer with open metal sites in the cylindrical cavities of the desolvated framework, *Chem. Commun.*, 2006, 959.

9 S. Xiang, W. Zhou, J. M. Gallegos, Y. Liu and B. Chen, Exceptionally High Acetylene Uptake in a Microporous Metal−Organic Framework with Open Metal Sites, *J. Am. Chem. Soc.*, 2009, **131**, 12415–12419.

10 Y. Ji, L. Ding, Y. Cheng, H. Zhou, S. Yang, F. Li and Y. Li, Understanding the Effect of Ligands on C2H2 Storage and C2H2/CH4 , C2H2/CO2 Separation in Metal–Organic Frameworks with Open Cu(II) Sites, *J. Phys. Chem. C*, 2017, **121**, 24104–24113.

11 H.-H. Wang, L.-N. Jia, L. Hou, W. Shi, Z. Zhu and Y.-Y. Wang, A New Porous MOF with Two Uncommon Metal–Carboxylate–Pyrazolate Clusters and High CO2/N2 Selectivity, *Inorg. Chem.*, 2015, **54**, 1841–1846.

12 K. Munusamy, G. Sethia, D. V. Patil, P. B. Somayajulu Rallapalli, R. S. Somani and H. C. Bajaj, Sorption of carbon dioxide, methane, nitrogen and carbon monoxide on MIL-101(Cr): Volumetric measurements and dynamic adsorption studies, *Chem. Eng. J.*, 2012, **195–196**, 359–368.

13 V. I. Agueda, J. A. Delgado, M. A. Uguina, P. Brea, A. I. Spjelkavik, R. Blom and C. Grande, Adsorption and diffusion of H2 , N2 , CO, CH4 and CO2 in UTSA-16 metal-organic framework extrudates, *Chem. Eng. Sci.*, 2015, **124**, 159–169.

14 O. I. Lebedev, F. Millange, C. Serre, G. Van Tendeloo and G. Férey, First Direct Imaging of Giant Pores of the Metal−Organic Framework MIL-101, *Chem. Mater.*, 2005, **17**, 6525–

6527.

15 Xiang, Wu, Zhang, Fu, Hu and Zhang, A 3D Canted Antiferromagnetic Porous Metal−Organic Framework with Anatase Topology through Assembly of an Analogue of Polyoxometalate, *J. Am. Chem. Soc.*, 2005, **127**, 16352–16353.

16 P. Mishra, S. Edubilli, B. Mandal and S. Gumma, Adsorption of CO2, CO, CH4 and N2 on DABCO based metal organic frameworks, *Microporous Mesoporous Mater.*, 2013, **169**, 75–80.

17 P. Mishra, S. Mekala, F. Dreisbach, B. Mandal and S. Gumma, Adsorption of CO2, CO, CH4 and N2 on a zinc based metal organic framework, *Sep. Purif. Technol.*, 2012, **94**, 124–130.

18 H. K. Chae, D. Y. Siberio-Pérez, J. Kim, Y. Go, M. Eddaoudi, A. J. Matzger, M. O'Keeffe and O. M. Yaghi, A route to high surface area, porosity and inclusion of large molecules in crystals, *Nature*, 2004, **427**, 523–527.

19 P. Maniam and N. Stock, Investigation of Porous Ni-Based Metal–Organic Frameworks Containing Paddle-Wheel Type Inorganic Building Units via High-Throughput Methods, *Inorg. Chem.*, 2011, **50**, 5085–5097.

20 Y. Kim, R. Haldar, H. Kim, J. Koo and K. Kim, The guest-dependent thermal response of the flexible MOF Zn2(BDC)2(DABCO), *Dalt. Trans.*, 2016, **45**, 4187–4192.

21 Y. He, J. Shang, Q. Gu, G. Li, J. Li, R. Singh, P. Xiao and P. A. Webley, Converting 3D rigid metal–organic frameworks (MOFs) to 2D flexible networks via ligand exchange for enhanced CO2/N2 and CH4 /N2 separation, *Chem. Commun.*, 2015, **51**, 14716–14719.

22 Z. Zhang, S. Xian, Q. Xia, H. Wang, Z. Li and J. Li, Enhancement of CO2 Adsorption and CO2/N2 Selectivity on ZIF-8 via Postsynthetic Modification, *AIChE J.*, 2013, **59**, 2195–2206.

23 R. Banerjee, H. Furukawa, D. Britt, C. Knobler, M. O'Keeffe and O. M. Yaghi, Control of pore size and functionality in isoreticular zeolitic imidazolate frameworks and their carbon dioxide selective capture properties., *J. Am. Chem. Soc.*, 2009, **131**, 3875–7.

24 D. W. Lewis, A. R. Ruiz-Salvador, A. Gómez, L. M. Rodriguez-Albelo, F.-X. Coudert, B. Slater, A. K. Cheetham and C. Mellot-Draznieks, Zeolitic imidazole frameworks: structural and energetics trends compared with their zeolite analogues, *CrystEngComm*, 2009, **11**, 2272.

25 R. Banerjee, A. Phan, B. Wang, C. Knobler, H. Furukawa, M. O'Keeffe and O. M. Yaghi, High-throughput synthesis of zeolitic imidazolate frameworks and application to CO2 capture., *Science*, 2008, **319**, 939–43.

26 F. V. S. Lopes, C. A. Grande, A. M. Ribeiro, J. M. Loureiro, O. Evaggelos, V. Nikolakis and A. E. Rodrigues, Adsorption of H2, CO2, CH4, CO, N2 and H2O in Activated Carbon and Zeolite for Hydrogen Production, *Sep. Sci. Technol.*, 2009, **44**, 1045–1073.

27 Z. Liu, L. Wang, X. Kong, P. Li, J. Yu and A. E. Rodrigues, Onsite CO2 Capture from Flue Gas by an Adsorption Process in a Coal-Fired Power Plant, *Ind. Eng. Chem. Res.*, 2012, **51**, 7355–7363.

28 B. J. Maring and P. A. Webley, A new simplified pressure/vacuum swing adsorption model for rapid adsorbent screening for CO2 capture applications, *Int. J. Greenh. Gas Control*, 2013, **15**, 16–31.

29 P. Xiao, J. Zhang, P. Webley, G. Li, R. Singh and R. Todd, Capture of CO2 from flue gas streams with zeolite 13X by vacuum-pressure swing adsorption, *Adsorption*, 2008, **14**, 575–582.

30 J. R. Rumble, Ed., in *CRC Handbook of Chemistry and Physics, 100th Edition (Internet Version 2019)*, CRC Press/Taylor & Francis, Boca Raton, FL, 2019.

31 B. T. Goodman, W. V. Wilding, J. L. Oscarson and R. L. Rowley, Use of the DIPPR Database for Development of Quantitative Structure−Property Relationship Correlations: Heat Capacity of Solid Organic Compounds †, *J. Chem. Eng. Data*, 2004, **49**, 24–31.

32 Pfeiffer Vacuum GmbH, Okta 4000, Roots pump, 400/690V, 50z|460V, 60 Hz, https://static.pfeiffer-vacuum.com/productPdfs/PPW71000.en.pdf, (accessed 8 April 2019).

33 Pfeiffer Vacuum GmbH, Okta 18000, Roots pump, 400/690V, 50 Hz|460V, 60 Hz, https://static.pfeiffer-vacuum.com/productPdfs/PPW90000.en.pdf, (accessed 8 April 2019).

34 GPSA, *Engineering Data Book*, Gas Processors Suppliers Association, Tulsa, OK, 12th edn., 2004.

35 Standards Australia, *AS1210-2010 Pressure vessels*, Australia, 2015.

36 D. J. Brennan, *Process Industry Economics: An International Perspective*, IChemE, Rugby, UK, 1997.

37 D. J. Brennan and K. A. Golonka, New Factors for Capital Cost Estimation in Evolving Process Designs, *Chem. Eng. Res. Des.*, 2002, **80**, 579–586.

38 M. Peters, K. Timmerhaus and R. West, *Plant Design and Economics for Chemical Engineers*, McGraw-Hill Education, 5th edn., 2003.

39 McGraw-Hill, Equipment Costs, http://www.mhhe.com/engcs/chemical/peters/data/, (accessed 24 May 2019).

40 D. E. Garrett, *Chemical Engineering Economics*, van Nostrand Reinhold, New York, 1989.

41 P.-E. Just, Advances in the development of CO2 capture solvents, *Energy Procedia*, 2013, **37**, 314–324.

42 A. Kohl and R. Nielsen, *Gas Purification*, Gulf Publishing Company, Houston, 5th edn., 1997.

43 E. W. Lemmon, M. O. McLinden and D. G. Friend, in *NIST Chemistry WebBook, NIST Standard Reference Database Number 69*, eds. P. J. Linstrom and W. G. Mallard, National Institute of Standards and Technology, Gaithersburg, MD, 2016.

44 J. Gabrielsen, M. L. Michelsen, E. H. Stenby and G. M. Kontogeorgis, A Model for Estimating CO2 Solubility in Aqueous Alkanolamines, *Ind. Eng. Chem. Res.*, 2005, **44**, 3348–3354.

45 H. Z. Kister, P. M. Mathias, D. E. Steinmeyer, W. Roy Penney, V. S. Monical and J. R. Fair, in *Perry's Chemical Engineers' Handbook*, eds. D. W. Green and M. Z. Southard, McGraw-Hill, New York, 9th edn., 2019.

46 C. Wang, M. Perry, F. Seibert and G. Rochelle, Packing Characterization for Post Combustion CO2 Capture: Mass Transfer Model Development, *Energy Procedia*, 2014, **63**,

1727–1744.

47 J. A. Rocha, J. L. Bravo and J. R. Fair, Distillation Columns Containing Structured Packings: A Comprehensive Model for Their Performance. 2. Mass-Transfer Model, *Ind. Eng. Chem. Res.*, 1996, **35**, 1660–1667.

48 H. Z. Kister, J. Sherffius, K. Afshar and E. Abkar, *Chem. Eng. Prog.*, 2007, 28–38.

49 M. T. Mota-Martinez, J. P. Hallett and N. Mac Dowell, Solvent selection and design for CO2 capture – how we might have been missing the point, *Sustain. Energy Fuels*, 2017, **1**, 2078–2090.

50 C. R. Wilke and P. Chang, Correlation of diffusion coefficients in dilute solutions, *AIChE J.*, 1955, **1**, 264–270.

51 R. M. DiGuilio, R. J. Lee, S. T. Schaeffer, L. L. Brasher and A. S. Teja, Densities and viscosities of the ethanolamines, *J. Chem. Eng. Data*, 1992, **37**, 239–242.

52 D. M. Newitt, M. U. Pai, N. R. Kuloor and J. A. W. Huggill, in *Thermodynamic Functions of Gases*, ed. F. Din, Butterworths Scientific Publications, London, UK, 1st edn., 1956.

53 D. E. Penny and T. J. Ritter, Kinetic study of the reaction between carbon dioxide and primary amines, *J. Chem. Soc. Faraday Trans. 1 Phys. Chem. Condens. Phases*, 1983, **79**, 2103.

54 A. Penttilä, C. Dell'Era, P. Uusi-Kyyny and V. Alopaeus, The Henry's law constant of N2O and CO2 in aqueous binary and ternary amine solutions (MEA, DEA, DIPA, MDEA, and AMP), *Fluid Phase Equilib.*, 2011, **311**, 59–66.

55 M. G. Shi and A. Mersmann, Effective Interfacial Area in Packed Columns, *Ger. Chem. Eng.*, 1985, **8**, 87–96.

56 G. Vázquez, E. Alvarez, J. M. Navaza, R. Rendo and E. Romero, Surface Tension of Binary Mixtures of Water + Monoethanolamine and Water + 2-Amino-2-methyl-1-propanol and Tertiary Mixtures of These Amines with Water from 25 °C to 50 °C, *J. Chem. Eng. Data*, 1997, **42**, 57–59.

57 A. Rix and Z. Olujic, Pressure drop of internals for packed columns, *Chem. Eng. Process. Process Intensif.*, 2008, **47**, 1520–1529.

58 A. E. Setekleiv and H. F. Svendsen, Dry pressure drop in spiral wound wire mesh pads at low and elevated pressures, *Chem. Eng. Res. Des.*, 2016, **109**, 141–149.

59 Sulzer Ltd., Gas/Liquid Separation Technology, https://www.sulzer.com/-/media/files/products/separation-technology/feed-inlet-devices/gas_liquid_separation_technology.ashx, (accessed 28 March 2019).

60 Y. Artanto, J. Jansen, P. Pearson, T. Do, A. Cottrell, E. Meuleman and P. Feron, Performance of MEA and amine-blends in the CSIRO PCC pilot plant at Loy Yang Power in Australia, *Fuel*, 2012, **101**, 264–275.

61 T. G. Amundsen, L. E. Øi and D. A. Eimer, Density and Viscosity of Monoethanolamine + Water + Carbon Dioxide from (25 to 80) °C, *J. Chem. Eng. Data*, 2009, **54**, 3096–3100.

62 Fläkt Woods AB, PFT - Two stage axial fan, http://resources.flaktwoods.com/Perfion/File.aspx?id=a3b52fc6-ca01-423f-bc28-1e1473b4efa0, (accessed 28 March 2019).

63 C. Wang, A. F. Seibert and G. T. Rochelle, Packing characterization: Absorber economic

analysis, *Int. J. Greenh. Gas Control*, 2015, **42**, 124–131.

64 W. M. Vatavuk, *Estimating Costs of Air Pollution Control*, CRC Press, 1st edn., 1990.

65 A. B. Corripio, K. S. Chrien and L. B. Evans, Estimate costs of heat exchangers and storage tanks via correlations, *Chem. Eng.*, 1982, 125–127.

66 The Sherwin-Williams Company, Standard API Tank Sizes, https://protective.sherwin-williams.com/pdf/tools-charts-list/standard_api_tank_sizes.pdf, (accessed 29 March 2019).

67 P. Suess and L. Spiegel, Hold-up of mellapak structured packings, *Chem. Eng. Process. Process Intensif.*, 1992, **31**, 119–124.

68 D. G. Chapel, C. L. Mariz and J. Ernest, in *Canadian Society of Chemical Engineers Annual Meeting*, Canadian Society of Chemical Engineers, Saskatoon, Saskatchewan, 1999.